

Evolution of physical and mechanical properties during phase transformation in poly(1-butene)

Bc. Kristýna Montágová

Master Thesis
2009

 **Tomas Bata University in Zlín**
Faculty of Technology

nascannované zadání s. 1

nascannované zadání s. 2

ABSTRAKT

Diplomová práce se zabývá studiem vývoje fyzikálních a mechanických vlastností izotaktického poly(1-butenu) (PB-1). Tento vývoj byl sledován v průběhu fázové transformace (PB-1) z nestabilní fáze II do termodynamicky stabilní fáze I. V této práci byly použity tři různé druhy PB-1 – dva homopolymery a jeden etylénový kopolymer, ze kterých byly lisováním a vytlačováním připraveny vzorky. Takto připravené vzorky byly temperovány při pěti různých teplotách po určitou dobu.

Pomocí širokoúhlé rentgenografie byl spočítán obsah fází ve vzorcích během fázové transformace; fyzikální vlastnosti byly měřeny změnou hustoty vzorků a změny mechanických vlastností byly měřeny tahovými zkouškami.

Bylo potvrzeno, že během fázové transformace dochází ke zvýšení hustoty a modulu pružnosti v tahu, přičemž temperační teplota má významný vliv na rychlost transformace.

Klíčová slova:

Poly(1-buten), fázová transformace, fyzikální vlastnosti, mechanické vlastnosti.

ABSTRACT

Master Thesis is focused on study of evolution of the physical and mechanical properties of poly(1-butene) (PB-1). This evolution was observed during the phase transformation from the metastable form II to the thermodynamically more stable form I. Three different commercially-available grades of PB-1 were used in this work; two homopolymers and one ethylene copolymer. Specimens were prepared via extrusion and compression-molding. Then these specimens were annealed at five various temperatures during a time.

Content of the form I in specimens was calculated by wide angle X-ray scattering during the phase transformation; physical properties were measured via density changes of specimens and changes of mechanical properties were measured via tensile testing.

It was proven that during the phase transformation density and tensile modulus increase in time and annealing temperature has significant effect on the transformation rate.

Keywords:

Poly(1-butene), phase transformation, physical properties, mechanical properties.

Acknowledgement

First of all I want to thank my parents for their support and interest during all my studies. I can not omit Jan Berka for his support and patience.

My great thanks also belong to Lubomír Beníček for his professional leadership and encouragement, valuable advice and suggestions during my work on this Thesis. Finally I also thank to Lenka Chvátalová for her assistance with tensile testing.

I declare, I worked on this Master Thesis by myself and I mentioned all the used literature.

Zlín, May 15, 2009

Kristýna Montágová

CONTENT

INTRODUCTION	9
I THEORETICAL BACKGROUND.....	10
1 POLY(1-BUTENE)	11
1.1 MOLECULAR STRUCTURE	11
1.2 SUPERMOLECULAR STRUCTURE.....	14
1.2.1 Form I.....	14
1.2.2 Form II	15
1.2.3 Form III	16
1.2.4 Forms I' and II'	17
1.3 CRYSTALLIZATION OF POLY(1-BUTENE).....	18
1.4 POLYMORPHIC TRANSFORMATION.....	20
1.4.1 Transformation of form II → I.....	22
2 PROPERTIES OF POLY(1-BUTENE)	25
2.1 PHYSICAL PROPERTIES	25
2.2 MECHANICAL PROPERTIES.....	25
2.3 APPLICATIONS.....	27
3 EXPERIMENTAL TECHNIQUES.....	28
3.1 DENSITY MEASUREMENT	28
3.2 X-RAY DIFFRACTION	28
3.2.1 Bragg's law	29
3.2.2 Wide angle x-ray scattering	30
3.3 TENSILE TESTING.....	30
3.4 EXTRUSION	32
3.5 COMPRESSION MOULDING	33
II EXPERIMENTAL BACKGROUND	34
4 MATERIALS.....	35
4.1 PB-0300M	35
4.2 DP0401M	36
4.3 PB-8640M	35
5 SPECIMENS PREPARATION	37
5.1 COMPRESSION MOLDING	37
5.2 EXTRUSION	37
5.3 ANNEALING.....	37
6 ANALYSING METHODS AND DEVICES	38
6.1 DENSITY MEASUREMENT	38
6.2 X-RAY DIFFRACTION	38
6.3 TENSILE TESTING.....	40
III RESULTS AND DISCUSSION.....	41
7 DENSITY MEASUREMENT.....	42
8 WIDE ANGLE X-RAY DIFFRACTION.....	46

9	TENSILE TESTING	47
9.1	MODULUS	47
9.2	YIELD STRESS.....	52
9.3	TENSILE STRENGTH AT BREAK.....	55
9.4	ELONGATION AT BREAK	58
	CONCLUSION	61
	REFERENCES	63
	LIST OF SYMBOLS	66
	LIST OF FIGURES	68
	LIST OF TABLES	70
	LIST OF EQUATIONS	71

INTRODUCTION

During the last century and a half, two new closely related classes of material have been introduced which have not only challenged the older materials for their well-established uses but they have also brought new products which have helped to extend the range of activities of mankind. Without these two groups of materials, rubbers and plastics, it would be difficult to conceive how everyday features of modern life such as automobile, telephone, television set and other could ever be developed [1].

Plastics are polymeric materials, which have high molecular weight substances with molecules resembling linear, branched, crosslinked, or otherwise shaped chains consisting repeating molecular groups. Synthetic polymers are prepared by polymerization of one or more monomers [2].

This Master thesis deals with isotactic poly(1-butene). PB-1 belongs to group polyolefins which are a large class of carbon-chain elastomeric and thermoplastic polymers usually prepared by addition (co)polymerization of olefins or alkenes such as ethylene [2].

Natta et al. investigated the polymerization of 1-butene in the same period as polypropylene was synthesized. They succeeded in producing PB-1 in 1954 and determined its crystal structure to prove its stereoregularity. It was characterized by peculiar polymorphic characteristic where it initially crystallized into the form II and then, within hours, recrystallizes into the form I [3]. Polymorphic property means that there is an existence of chemical substances in two (dimorphism) or more physical forms [4]. Poly(1-butene) exhibits five crystal modifications depending on the crystallization conditions: form I - twined hexagonal with $3/1$ helix; form II - tetragonal with $11/3$ helix; forms I' and II' - untwined hexagonal; form III - orthorhombic with $4/1$ helix [5, 6].

The aim of this work is to describe evolution of the physical and mechanical properties during phase transformation. For this purpose, three grades of PB-1 produced by Basell Polyolefins, Louvain la Neuve, Belgium were used. Specimens designed for observation of evolution of physical and mechanical properties were prepared via extrusion and compression molding. Accordingly to the aim, following experimental techniques were used: density measurement, wide angle X-ray scattering and tensile testing.

I. THEORETICAL BACKGROUND

1 POLY(1-BUTENE)

1.1 Molecular structure

Poly(1-butene) is a thermoplastic polymer and due to using stereospecific Ziegler-Natta catalysts belongs to the family of polyolefins (Figure 1) [7].

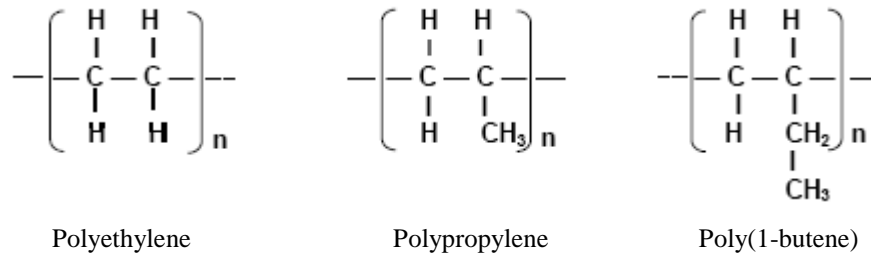


Figure 1. Structure of various polyolefins [7]

Poly(1-butene) is relatively unexplored polyolefin which shares many features in common conventional polyolefins like polypropylene and polyethylene, while at the same time offering versatility, value and opportunity through a range of properties not usually associated with this polyolefins [8].

Poly(1-butene) is obtained by polymerization of butene-1, with stereospecific Ziegler-Natta catalyst (Figure 2) to create a linear, high molecular, isotactic, semicrystalline polymer [8]. Natta and coworker first synthesized PB-1 in 1954 using two-component catalyst systems containing organoaluminum compounds and transition metal salts and halides. Subsequent modifications to the original Ziegler-Natta catalytic systems by other researchers helped to improve the degree of isotacticity [6].

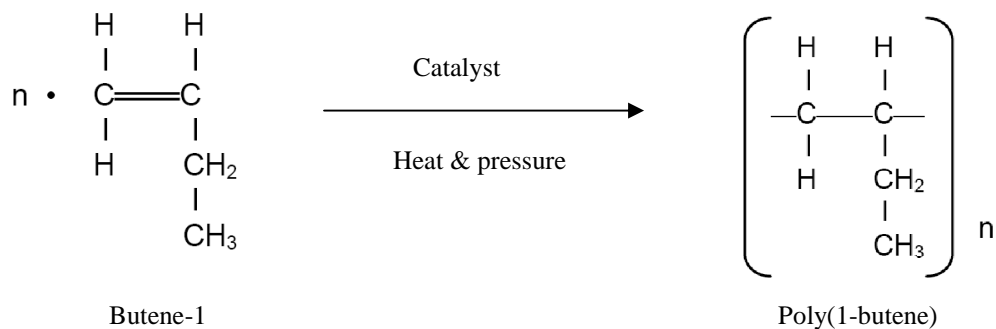


Figure 2. Producing reaction of poly(1-butene) [8]

The isotacticity of PB-1 can be quantified by several methods. These methods include selective solvent extraction, infrared spectroscopy, X-ray diffraction and nuclear magnetic resonance (NMR) spectroscopy [9]. PB-1 is a highly isotactic, partially crystalline homopolymer of high molecular mass. Highly isotactic means that nearly all C2 side chains are attached to the same side of the molecule. PB-1 must not be confused with the rubber-like polyisobutene [7].

Poly(1-butene) was usually formed by Ziegler–Natta type catalyst as it is mentioned above. In recent decades, a new kind of homogeneous Ziegler–Natta catalyst composed group of IVB metallocene and methylaluminoxane (MAO) which has been used for the stereospecific polymerization of α -olefins. Different stereospecific arrangements of poly(1-butene) can be produced owing to the steric and electronic effects of the cyclopentadienyl ligands of the metallocenes. The nature of the transition metal as well as the ligand type of the catalyst controls the catalytic activity and the stereoregularity of poly(1-butene). PB-1 (Figure 3) can be obtained by stereorigid chiral *ansa*-metallocene catalysts with C_2 symmetry, such as *rac*-Et(Ind)₂ZrCl₂ and CH₂(Ind)₂Ti(CH₃)₂ [10, 11]. While those with bilateral symmetry, *i*-Pr(Cp)(Flu)ZrCl₂, Me(Cp)(Flu)ZrCl₂, and CH₃CH(Cp)(Flu)ZrCl₂, produce syndiotactic poly(1-butene). Achiral and symmetric metallocenes are non-stereospecific and generally produce an atactic poly(1-butene) [11].

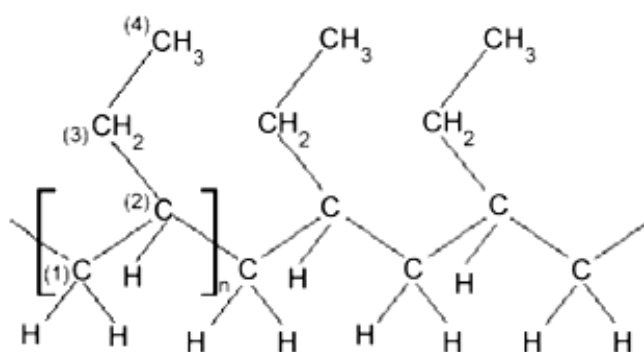


Figure 3. The chemical structure of the isotactic poly(1-butene) [12]

For a given chemical structure, the main contribution to the line position is due to conformations and it is referred in the literature as the γ -gauche effect. The position of the lines can be determined with an *ab initio* calculation. Often, already a semiempirical approach is sufficient to depict the observed chemical shifts. The line position of a given

^{13}C is influenced by the distance to the neighboring ^{13}C in the γ position. The value of the dihedral angle about a single bond controls the distance between a carbon and its γ neighbor. When the conformation about the bond passes from trans (t) to gauche (g), the distance (respective interaction) between these atoms is reduced (respective increased), and the peaks are shifted by a value of up to -5ppm. Shielding effects vary with dihedral angle and are, in general additive [9].

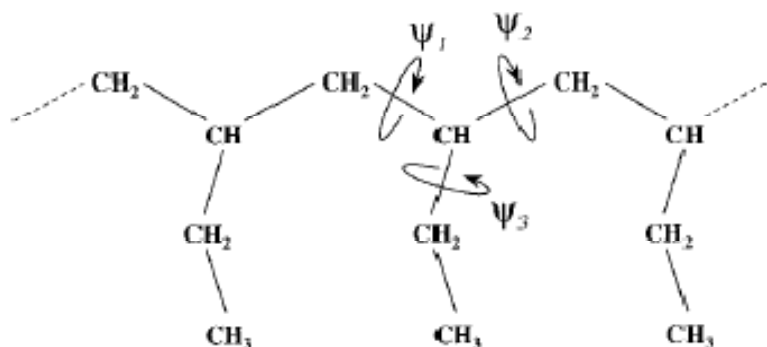


Figure 4. Definition of the dihedral angles in PB-1 [9]

The three internal rotation angles ψ_1 , ψ_2 , and ψ_3 , characterizing the carbon chain conformation of PB-1, are represented in Figure 4 [9].

1.2 Supermolecular structure

Isotactic poly(1-butene) has a very complex polymorphic behavior, since it can crystallize into various crystalline forms, depending on preparation conditions. The three main polymorphs, forms I, II, and III, correspond to different mode of chain packing with different helix conformations. But five different crystalline modifications have been reported in the literature, which are referred to as I, II, III, I', and II' [6, 9, 13].

Polymorphism means the existence of chemical substances in two (dimorphism) or more physical forms [4]. PB-1 is polymorphic material occurring in five crystallographic modifications [14], but only the tetragonal form II and the hexagonal form I, are of practical interest [15]. Structural characteristics are resumed in Table 1.

Table 1. Structural characteristics for the crystal modifications of PB-1 [5]

form	crystal lattice	helix	Unit cell dimensions (nm)			T_m (°C)
			<i>a</i>	<i>b</i>	<i>c</i>	
I	hexagonal (twined)	3/1	1.77	1.77	0.65	125–135
I'	hexagonal (untwined)	3/1	1.77	1.77	0.65	90–100
II	tetragonal	11/3	1.46	1.46	2.12	110–120
III	orthorombic	4/1	1.25	0.89	0.76	90–100

1.2.1 Form I

Modification of the form I is hexagonal [16]. The chains adopt left-handed 3/1 helix conformation packed in a trigonal lattice [9].

On the basis of wide angle X-ray scattering (WAXS) measurements and helix packing energy calculations, three different 3/1 helix arrangements were proposed for the form I (see Figure 5):

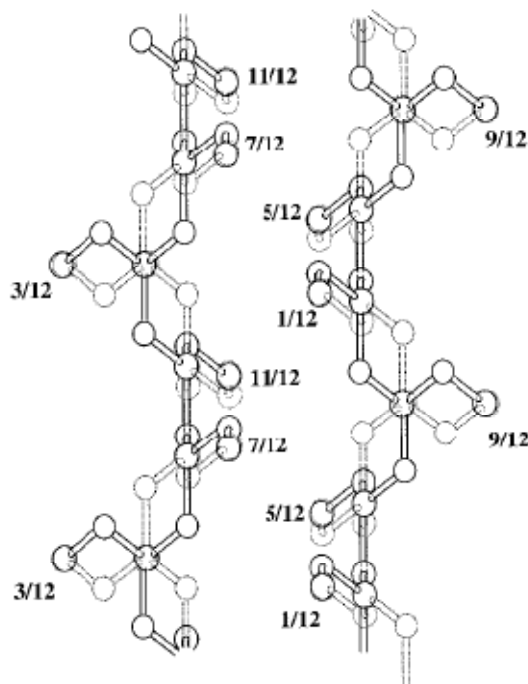


Figure 5. *3/1 helix packing in form I. Pair of isoclined helices: Two full (or two dotted) neighboring helices; pair of anticlined helices: One dotted helix surrounding one full helix [9]*

Winkel and Miles [17] studied the surface of ultra-thin PB-1 and used an atomic force microscope (AFM). It is known that the tetragonal form II is unstable, converting over time to the most prevalent form I. Comparison of the images with other studies surfaces enabled identification of which plane of which form was observed in the AFM images. The specimens were prepared in such a way that the bulk would be in the stable phase. They found that this form is also stable on the surface [17].

1.2.2 Form II

In the crystalline domains of form II, 11/3 helices are packed in a tetragonal symmetry [9]. This packing produces a different chemical environment for each monomer carbon in the unit cell (see Figure 6) and therefore, it should result in a multiple splitting or a broadening of the lines. Nevertheless, this broadening should not exceed 1ppm. As indicated before, the spectrum of the form II not only corresponds to chains in the crystalline domains but also in the amorphous domains. Hence, one would expect to get a superposition of a broad spectrum arising from the multiple frozen backbone

and side-chain conformations in the amorphous domains and a well-resolved spectrum arising from the crystalline domains. No sharp line is observed for the methane suggests that there is a distribution of backbone conformations in the crystalline domains as well because the CH resonance is sensitive to the torsion angles ψ_1 and ψ_2 . Such a distribution of torsion angles along the backbone of the polymer is rather unusual in the crystal [9].

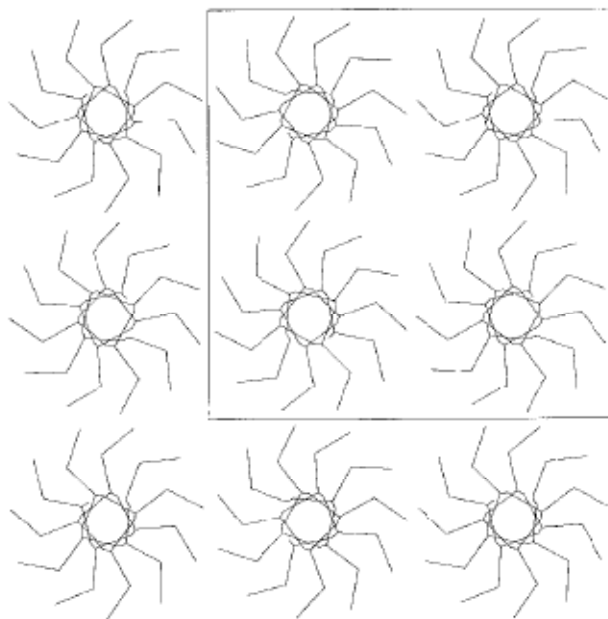


Figure 6. Projection of the structure of PB-1 form II on the (001) plane [9]

1.2.3 Form III

The form III, which is obtained from crystallization from solution by evaporation of the solvent, consists of helices of a single chirality with 4/1 symmetry packed in an orthorhombic lattice [9].

As in the form I, the splittings of the lines can also be explained in terms of inter-chain environments. That the symmetry of the helices does not reflect the symmetry of the space group gives rise to nonequivalent positions for the carbons, as illustrated in Figure 7. Repeating units experience two different environments. This leads to the splitting of all the resonances in a 1/1 ratio. The difference of the chemical shift of the splitting corroborates the hypothesis of an inter-chain effect. The side-chain carbons are more sensitive to the inter-chain environment than the backbone carbons; consequently, the related splitting is larger [9].

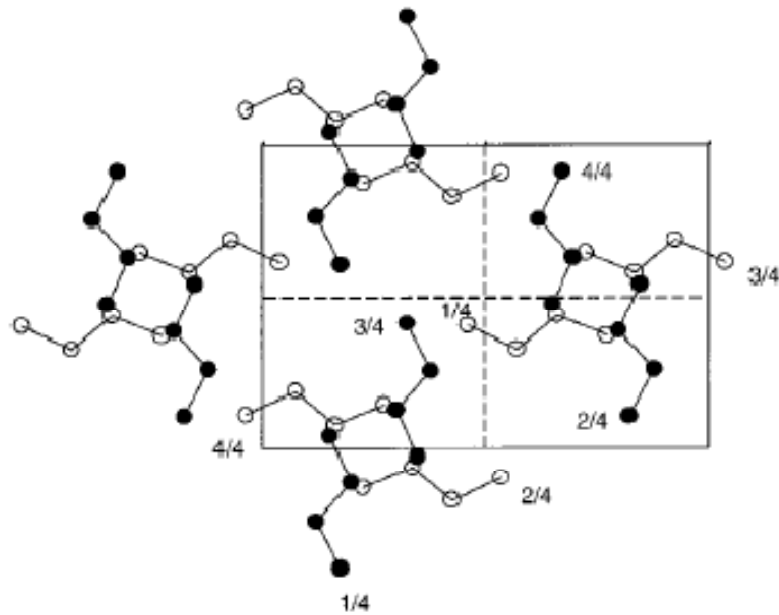


Figure 7. Projection of the structure of PB-1 form III on the (001) plane as determined by X-ray diffraction. Only carbons are represented. Black and white marked carbons experience different local environments [9]

1.2.4 Forms I' and II'

Structural analyses show that the form I crystals exhibit usually a twined hexagonal structure, while the form I' crystals occur in an untwined hexagonal form. The PB-1 chains possess the same 3/1 helical conformation in the both forms I and I' [18].

Nakafuku and Miyaki [6] studied the effect of pressure on the crystallization behavior of PB-1 and reported that its melt crystallization under high pressure produces the stable form I', which shows the same X-ray diffraction pattern as form I but has a much lower melting temperature (96 versus 130 °C) at atmospheric pressure. Above 200 MPa, the forms I' and II' are crystallized from the melt. The form II' shows the same X-ray diffraction pattern as form II, but a lower melting temperature than form II. The form II' is metastable at atmospheric pressure and transforms to the form I' on standing at room temperature [6].

1.3 Crystallization of poly(1-butene)

The crystallization behavior of thermoplastic polymers is strongly affected by processing conditions. The degree of crystallization and the size of the resulting spherulites depend on temperature and cooling rate. Furthermore, it is known that flow significantly enhance the kinetics of crystallization and to produce highly oriented morphologies. The global effect of flow on crystallization is often referred to flow-induced crystallization (FIC) [19].

The quality and quantity of crystallization, i.e., the number, size, shape, and crystalline form of the crystallites, depend on a number of different parameters and material properties. Among them, molecular weight (MW) and molecular weight distribution (MWD) are known to play an important role when FIC are considered [20].

Morphology of melt-crystallized PB-1 thin films was examined by means of AFM in tapping mode. It depends remarkably on the temperature of crystallization. When crystallizing the PB-1 at temperatures lower than 60 °C, spherulitic structures were observed. Flat-on lathlike crystals could be formed at temperatures higher than 90 °C. In the temperature range 60 – 90 °C, the spherulitic and flat-on lathlike structures coexist in the same specimen. Representative spherulitic AFM images of PB-1 thin films are shown in Figure 8. The PB-1 specimen was heat-treated at 160 °C for 5 min to erase possible effects of thermal history on its re-crystallization and subsequently cooled to room temperature in air. From both height (Figure 8 (a) and (c)) and phase (Figure 8 (b) and (d)) images, it can be recognized that the spherulites, with diameters typically measure from 10 to 20 μm , consist of packed closely edge-on crystalline lamellae grown from the central regions, i.e. the crystalline nuclei, continuously outward by splaying and branching. The lateral width of the PB-1 lamellae ranges from hundreds to thousands nanometers, while the average thickness of the PB-1 lamellae is measured to be ca. 30 nm. Moreover, there exist two different types of nuclei in the PB-1 spherulites. As shown in Figure 8 (a) and (b), the first type of spherulites exhibits two typical spherulitic ‘eyes’ on either side of the crystalline nuclei. In the second type of spherulites, Figure 8 (c) and (d), a leaf-like structure can be found at the center with various shapes. This kind of structure was also observed in the solution-cast thin films [18].

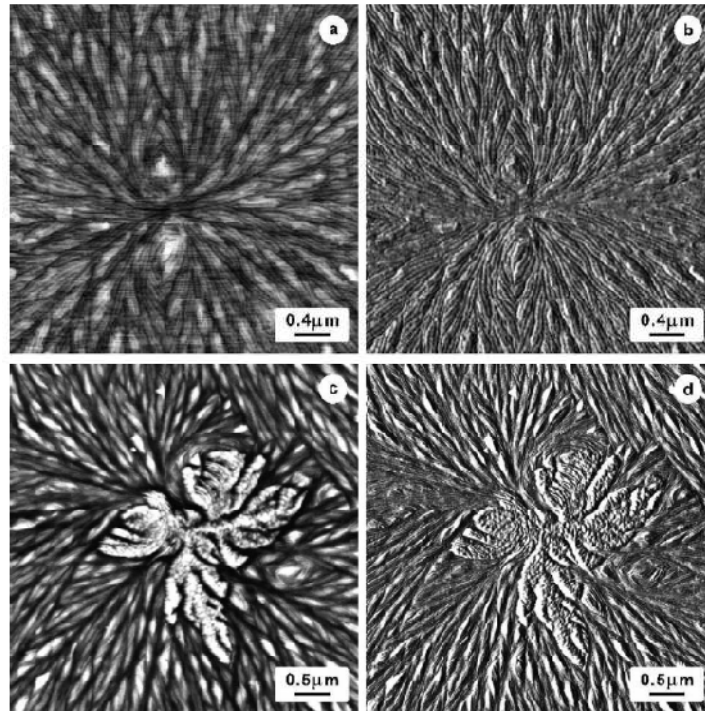


Figure 8. AFM height (a,c) and phase (b,d) images illustrates the two different kinds of PB-1 spherulites. The specimen was heat-treat at 160 °C for 5 min and then quenched to room temperature in air. [18]

Yan et al. [18] monitored the morphologies of melt crystallized PB-1 in ultra thin films by AFM in tapping mode. Combining the facts that nucleation of the stable form I crystals starts most likely at crystalline side surfaces or corners and that the phase conversion rate of the melt grown flat-on crystals is much faster than that of the solution grown single crystals, they speculated that residual local thermal stresses exist at the edges of the micro-crystallites and stacking regularity of the crystalline lamellae play a very important role in generating the nuclei of the form I crystals [18].

The appearance of the forms I' and II' is related to crystallization under high pressure which shows X-ray diffraction patterns similar to those of forms I and II, respectively, but with different dT_m/dP values. The line position in the high-resolution ^{13}C spectra of polyolefins in the solid state are determined by the intrinsic isotropic chemical shift of the functional group by the chain conformation and by inter-chain shielding contributions [9].

1.4 Polymorphic transformation

The most important phenomenon is the transformation of the form I into the form II, which takes place in PB-1 at room temperature after crystallization from the melt. Natta et al. were the first to discover that PB-1 assumes an 11/3 helical conformation with a tetragonal unit cell when crystallizing from the melt. This crystalline structure is known as form II. It is unstable and transforms into a stable 3/1 helix conformation (form I) with hexagonal (rhombohedral) unit cells at room temperature and atmospheric pressure. This transformation results in the desirable properties of the material. The melting point increases from 120 to 135 °C. The transformation is accelerated by the application of pressure of only a few tens MPa. The form III has been observed in films of PB-1 precipitated from certain solvents [6].

The polymorphic transformation of PB-1 increases the possible uses of this polymer. Firstly, properly molded and processed articles made from PB-1 show very good resistance to creep and environmental stress cracking. Secondly, extruded PB-1 is generally used in the manufacture of the pipes and tubes because its impact and corrosion resistance [12].

Poly(1-butene) generally crystallizes from the melt prevalently in the form II but, upon cooling, spontaneously transforms into the thermodynamically stable form I [15]. The kinetic of this transformation is being influenced by pressure, temperature, and mechanical deformation and has been extensively studied in the past via differential scanning calorimetry (DSC), WAXS, and small angle X-ray scattering (SAXS) [21]. This transformation takes about one week under normal conditions and it is reflected by important changes in the physical-mechanical properties. During the transformation from the form II to the form I density, crystallinity, hardness, rigidity, stiffness and tensile strength increase to values characteristic of the form I. The relatively constant values for ultimate tensile strength and elongation indicate that stretching or orientation accelerates the form II to the form I transformation [15].

Nakamura et al. [5] used PB-1 films, consisting either of crystal form III (solution-grown crystal) or form I' (melt-crystallized film under a high pressure), were drawn uniaxially by tensile draw and solid-state co-extrusion in the range of room temperature (RT) to 80 °C, below their melting temperatures ($T_m = 90 - 100$ °C). The phase transformations

induced by draw were characterized by WAXS and DSC. The results are discussed in terms of the effect of drawing variables on the deformation mechanism of PB-1 [5].

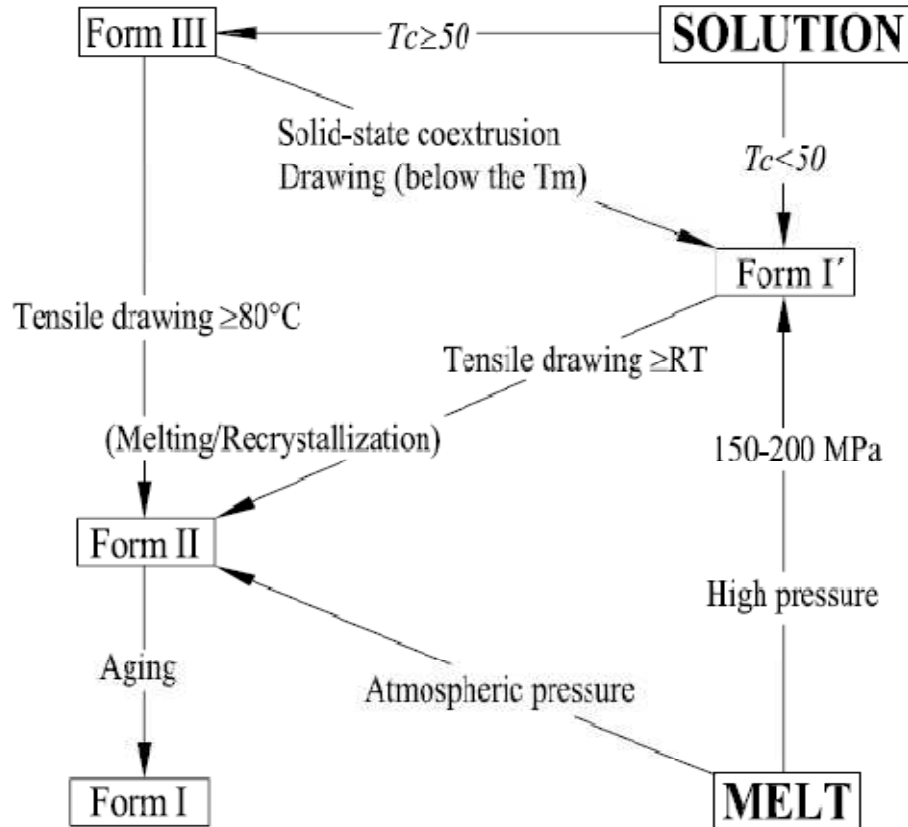


Figure 9. Schematics showing routes for the formation and transformation of crystal modifications on crystallization and drawing of PB-1 [5]

The phase transformation upon the drawing of PB-1 specimens with either form I' or form III is summarized in Figure 9. The drawing was made by solid-state co-extrusion and tensile drawing at RT to 80 °C. Drawing variables had a significant effect on the deformation mechanism. Solid-state co-extrusion of these specimens produced oriented tapes with the form I' independently of the initial crystal forms and co-extrusion temperatures, this probably means that the deformation proceeded in the crystalline state. The tensile draw of the form III at a higher T_d of 80 °C, near the T_m of 90 – 100 °C, produced an oriented tape with unstable form II crystals, which spontaneously transformed into the stable form I. However, the drawing of the form III at a lower T_d of 70 °C yielded an oriented tape with form I' crystals. In contrast to the form III, the tensile draw of the form I' was found

to produce oriented tapes with form II crystals independently of T_d , although the amount of form II crystals generated decreased with decreasing the T_d [5].

1.4.1 Transformation of form II \rightarrow I

Marigo et al. [15] studied these transitions which were carried out by different experimental techniques, such as WAXS and DSC, but the investigation of the lamellar structure of PB-1 by SAXS was unusual. Their work was concerned to the change of crystallinity and of the characteristic parameters of the lamellar stacks, during the phase transition II \rightarrow I, employing both WAXS and SAXS techniques. It was found that the interpretation of WAXS and SAXS data allows one to suppose that a twofold mechanism could be taking place during the phase transition II \rightarrow I in PB-1. The transition nucleation seems to be localized on lamellar distortion points, and the transition itself involves the rearrangement of lamellae and of lamellar stacks. Moreover, a further crystallization of the amorphous phase into the form I, seems to take place, with the appearance of new thin lamellae inside lamellar stacks [15].

The form II is kinetically favored. In this stage PB-1 is a rather soft, mechanically weak material. Over several days the material hardens by transforming into the form I which is thermodynamically favored. This crystalline transformation can be observed by DSC, as shown in Figure 10 [7].

This transformation depends strongly on ambient temperature and pressure as demonstrated in Figure 11. At atmospheric pressure (0.1 MPa) the maximum rate of transformation occurs around 20 °C but drops significantly by increasing or decreasing the temperature. If ageing is performed at lower or higher temperatures than 20 °C only the time to achieve final properties is longer: the final performance of the material itself is not affected [7].

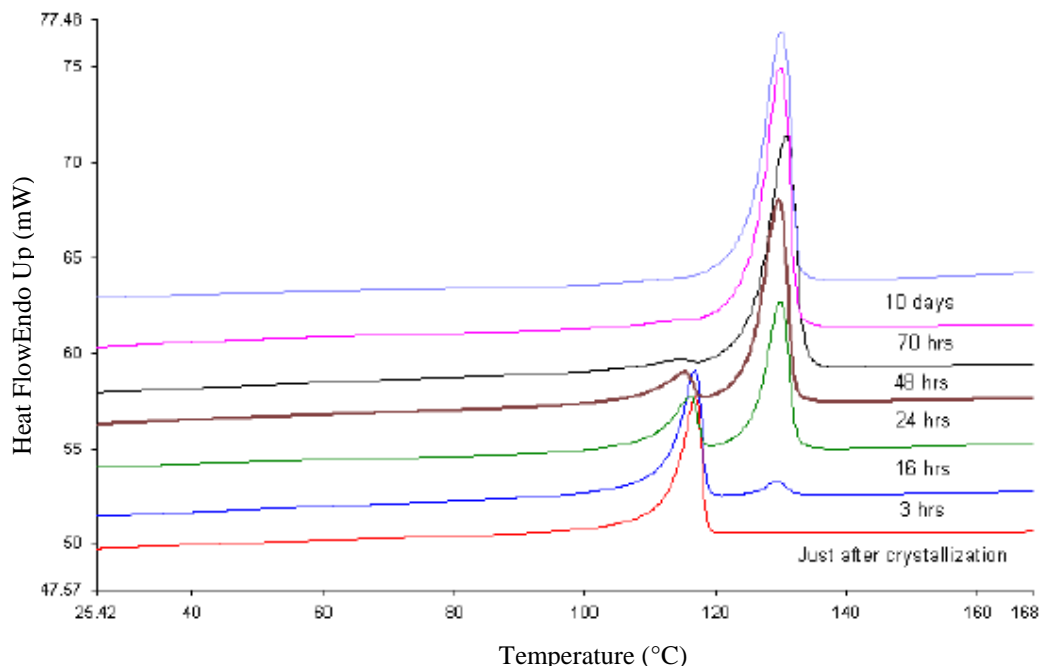


Figure 10. Transformation of the crystalline form II \rightarrow I of PB-1 produced by LyondellBasell [8]

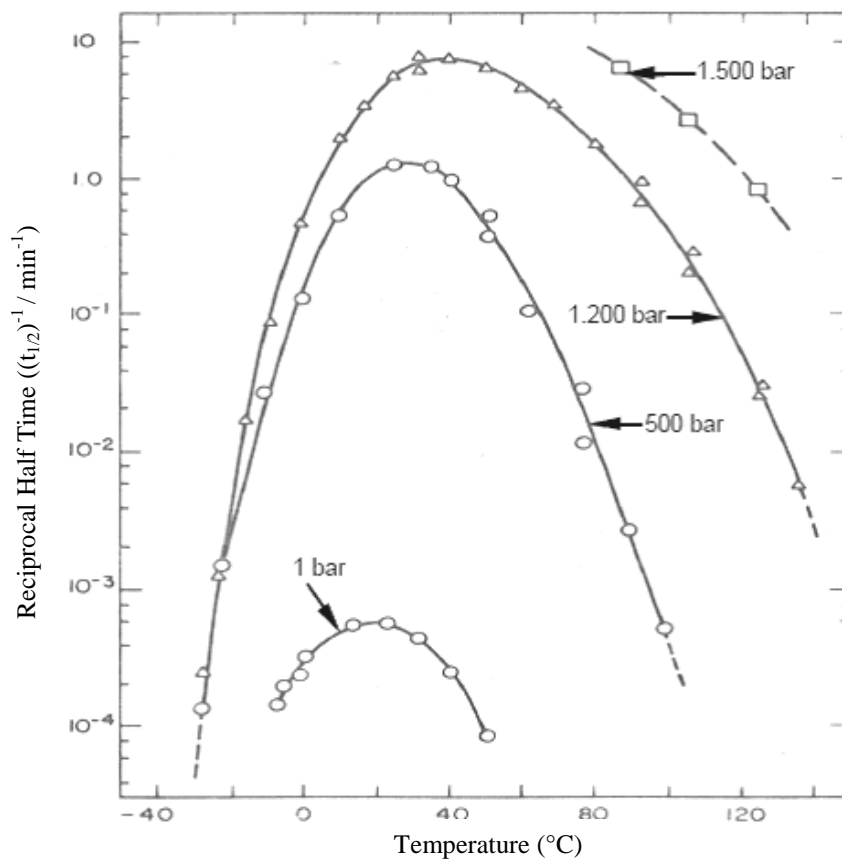


Figure 11. Dependence of transformation of the form II \rightarrow I of PB-1 on temperature and pressure [8]

As can be seen in Figure 11, the crystalline transformation can be shortened from a few days to only a few minutes by application of hydrostatic pressure of up to 200 MPa using a suitable autoclave. [8]

Only in this final stage after termination of ageing PB-1 achieves its excellent high temperature mechanical strength which for pipe and piping system producers makes the material a preferred candidate for all hot water applications. [7]

2 PROPERTIES OF POLY(1-BUTENE)

Poly(1-butene), similarly as polyethylene or polypropylene has a unique morphology and crystallization behavior combined with carefully controlled molecular parameters give PB-1 a profile of properties which combines typical features of conventional polyolefins and particular characteristics of technical polymers. PB-1 displays excellent resistance to creep, abrasion, chemicals and environmental stress cracking – these properties customers of LyondellBasell view as desirable in pipes for heating and plumbing. The very high molecular weight ($M_w = \text{ca. } 500.000$) and relatively long ethyl side groups of the polymer chains provide what are effectively very strong cross-links and a high number of tie molecules which help to maintain the network also at high temperatures close to the melting point [8].

Poly(1-butene) by nature displays excellent creep resistance. It does not require additional cross-linking or any other modification. The PB-1 crystallites act as fixed multi-functional cross-links that are supported by entanglements where extensive slipping is prevented by the ethyl side groups of the polymers [7].

2.1 Physical properties

Density and melt temperature of poly(1-butene) of several forms are shown in Table 2.

Table 2. Density and melt temperature of PB-1

Material	Density [g.cm ⁻³]	T _m [°C]	Ref.
PB-1 form I	0.950	125 – 135	[8]
PB-1 form II	0.900	110 – 120	[8]
PB-1 form III	0.897 ~ 0.906	90 – 100	[8, 22]
PB-1 amorphous	0.870		[8]

2.2 Mechanical properties

Poly(1-butene) is a partially crystalline polymer with high isotacticity and consequently high crystallinity. The crystalline fraction of semicrystalline polymer influences certain characteristics. Generally, increasing crystallinity raises stiffness, hardness, density, creep resistance, temperature resistance, abrasion resistance and lowers swelling by chemicals. The amorphous part determines characteristics like tensile and impact strength, crack

propagation, and stress cracking resistance [7, 8]. Mechanical properties of PB-1 are summarized in Table 3.

Table 3. Mechanical properties of PB-1 [7]

Material properties	Method	Unit	PB-1 4237
Tensile strength at yield	ISO R 527	MPa	20
Tensile strength at break	ISO R 527	MPa	35
Elongation at break	ISO R 527	%	300
Flexural Elastic Modulus	ISO R 178	MPa	450
Notched Impact Strength at 20 °C	ISO R 180	kJ.m ⁻²	20
Notched Impact Strength at 0 °C	ISO R 180	kJ.m ⁻²	7

The peculiar tensile behavior of PB-1 is based mainly on these chain entanglements. PB-1 does not show the typical necking behavior; instead it tends to support the load while it continues to stretch. Depending on the preparation of the test specimen and the conditions of measurements, PB-1 may exhibit a very little yielding (Figure 12) [7].

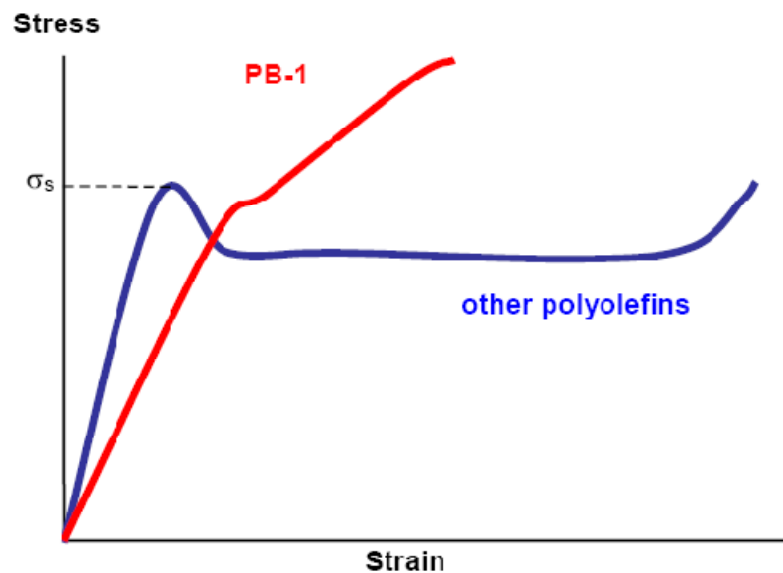


Figure 12. Tensile behavior of PB-1 vs. other polyolefins [7]

2.3 Applications

A major application area of PB-1 is in seal-peel or easy-open packaging. Typical examples include carton liners (e.g. cereal packaging) and packs for pre-packed delicatessen products like cold meats, cheeses and smoked salmon. PB-1 offers the ability to customize sealing temperatures and seal strength whilst giving consistent, reliable processing and sealing performance on existing equipment, and built-in tamper-evidence. Poly(1-butene) can also be used in film modification to increase flexibility and softness without sacrificing clarity. In a similar vein, PB-1 is used to modify polypropylene fibres to enhance softness, flexibility and to provide a unique feel [23].

This material is also used commercially in films that require creep resistance such as insulation compression packaging. It can also be used as a layer or overall film for hot filled heavy duty packaging, tapes for bundling and holding loads at elevated temperature such as bale wrap, special sheet applications such as anti-erosion geo-grids and netting and cable-ties. Features from PB-1 in hot melt adhesives, where its unique crystallization behavior reduces the melting point and extends the "open time" of the adhesive to as much as 30 minutes, to enable time for repositioning of components prior to setting. It is used widely as a component in hot melt adhesives for non-woven fibre webs [23].

Poly(1-butene) is also typically used in applications that see continuous load at moderate to high temperatures. It is used in electric domestic heaters in North America, where it is blow molded into large 15 ~ 20 kg tanks. Other logical extensions may include fire extinguishers, residential and swimming pool water filter housings, pressurized pneumatic holding tanks, hoses, compressed gas cylinders and aerosol dispensers, to name just a few. There is also considerable interest in the potential of PB-1 to be used as a component in synthetic wine corks.

It is also possible to employ PB-1 in compounded polymer products to provide unique benefits. It accepts extremely high filler loadings (>70%), which combined with its low melting point, enables it to be used in halogen-free flame retardant composites or as a master batch carrier for difficult-to-disperse or temperature-sensitive pigments; its unique rheology and concomitant easy dispersability enable it to be used at very low levels in other polyolefins as a processing aid to reduced extruder pressures and/or increase extruder throughput [23].

3 EXPERIMENTAL TECHNIQUES

3.1 Density measurement

Density is the concentration of matter, it is the amount of mass per unit volume of a substance. Iron has a greater density than wood, and wood has a greater density than styrofoam. The relative density (specific density) of a substance is a measure of how it compares in density to water. The vapor density of a gas is a measure of how it compares to the density of hydrogen at a particular pressure and temperature [24].

Density measurement is used for research of physical or molecular changes of materials structure. Density measurement is common to use for crystallinity degree of polymer determination, a well for filler content determination. Density of plastic can be depended on used conditioning or thermal material processing. Physical structure of polymer can be changed with time and temperature. Volume is depended as well on temperature. Consequently density can be a function of time and/or temperature [25].

Density determination of plastics has been fully performed in accordance to ČSN EN ISO 64 0111.

3.2 X-ray diffraction

X ray diffraction is a non destructive method of characterization of solid materials. X-ray scattering and diffraction are among the principal tools for studying polymers, with their utility proven since the very inception of polymer science [26, 27].

X-ray diffraction is one of the primary methods for determining macromolecular conformations in the crystalline solid state. The intramolecular conformational considerations for polymer chains in solution appear to be the dominant forces for determining solid-state conformations. However, in the solid state we must also consider the intermolecular requirements of chain packing. Crystal structures of polymers can also be used to establish the conformations of the crystalline regions of fluoro-polymers, the conformations of polymers that prefer gauche conformations (such as polyoxymethylene), and the conformations of stereoregular materials. Crystallography is also useful for determining the crystallization that occurs upon stretching rubbery polymers such as polyisobutylene or natural rubber [28].

X-rays are produced generally by either X-ray tubes or synchrotron radiation. In a X-ray tube, which is the primary X-ray source used in laboratory X-ray instruments, X-rays are generated when a focused electron beam accelerated across a high voltage field bombards a stationary or rotating solid target. As electrons collide with atoms in the target and slow down, a continuous spectrum of X-rays are emitted, which are termed Bremsstrahlung radiation. The high energy electrons also eject inner shell electrons in atoms through the ionization process. When a free electron fills the shell, an X-ray photon with energy characteristic of the target material is emitted. Common targets used in X-ray tubes include Cu and Mo, which emits 8 and 14 keV X-rays with corresponding wavelengths of 1.54 and 0.8 Å, respectively [29].

3.2.1 Bragg's law

The law enables the structure of many crystals to be determined. It was discovered in 1912 by Sir Lawrence Bragg, who was awarded the 1915 Nobel Prize for physics for their pioneering work on X-ray crystallography. A beam of X-rays (wavelength of the rays, λ) strikes a crystal surface in which the layers of atoms or ions are separated by a distance, the maximum intensity of the reflected ray occurs when:

$$\sin \theta = \frac{n\lambda}{2d} \quad (1)$$

(See Figure 13), where θ (known as the Bragg angle) is angle between the incident rays and the surface of the crystal, d is a distance and n is an integer [4, 30].

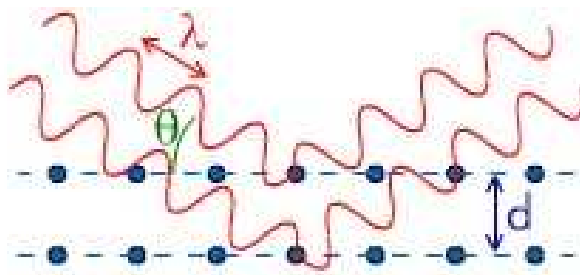


Figure 13. Bragg's law [30]

When an integer (1, 2, 3 etc.) the reflected waves from different layers are perfectly in phase with each other and produce a bright point on a piece of photographic film. Otherwise the waves are not in phase, and will either be missing or faint [30].

3.2.2 Wide angle X-ray scattering

Wide angle X-ray scattering is an X-ray diffraction technique that is often used to determine the crystalline structure of polymers. This technique specifically refers to the analysis of Bragg Peaks scattered to wide angles, which (by Bragg's law) implies that they are caused by sub-nanometer sized structures [26].

A diffraction technique for polycrystalline films where only crystallites diffract which are parallel to the substrate surface. The diffraction pattern generated allows to determine the chemical composition or phase composition of the film, the texture of the film (preferred alignment of crystallites), the crystallite size and presence of film stress. According to this method, the specimen is scanned in a wide angle X-ray goniometer, and the scattering intensity is plotted as a function of the 2θ angle. A crystalline solid consists of regularly spaced atoms (electrons) that can be described by imaginary planes. The distance between these planes is called the d-spacing. The intensity of the d-space pattern is directly proportional to the number of electrons (atoms) that are found in the imaginary planes [26].

3.3 Tensile testing

The mechanical behavior of a material extends from its stress/deformation response, in which the mode of deformation (uniaxial, biaxial, etc.) is particularly important to define, as are the loading profile and environment under which a given test is carried out. [31].

The mode of tensile deformation will be used to elucidate some of the important parameters describing the mechanical properties of a material. Figure 14, is a general sketch of a common stress/strain response exhibited by many polymeric materials particularly ductile semicrystalline materials like polyethylene or polypropylene. Often, extracted data that might help convey the mechanical response of the system and that may be useful in deciding on the applicability of a given material are the values of σ_b and ε_b

(see Figure 14) that will be of importance since these are related to the stress at break and to the strain at break, the latter of which can now easily be converted to percent elongation, the extension ratio, or true strain at break. The values σ_y and ε_y are particularly important and should be distinctly noted if this “peak” occurs in the stress/strain response. The respective stress and strain correlated with this peak are known as the yield stress and yield strain. These values are crucial, for they indicate the stress and strain beyond which a material will no longer return to its initial dimensions; that is, plastic deformation or permanent set will generally be induced in the material [31].

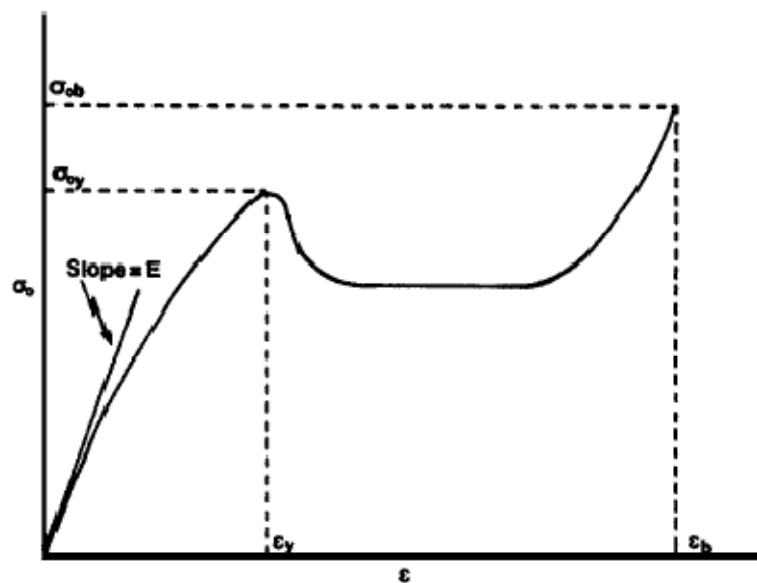


Figure 14. Generalized stress-strain curve that shows distinct yield [31]

Again referring to Figure 14, the region following the yield point might imply that “strain softening” is occurring, but this is often principally a result of the decrease in cross-sectional area and hence is not an entirely appropriate term to use for such behavior.

Very significant parameter (Figure 14) is the initial slope of the stress/strain curve. This slope is called Young’s modulus, the tensile modulus, or modulus of elasticity and is given the symbol E . By definition this can be written:

$$E = \lim_{\varepsilon \rightarrow 0} \left(\frac{d\sigma_0}{d\varepsilon_0} \right) \quad (2)$$

This parameter is an index of the stiffness of the material since it represents the stress generated in the limit of small deformation. This stiffness parameter is particularly

significant in this article. It might be pointed out that if the stress/strain curve displays an initial “toe” in its behavior prior to it displaying a linear region, this is often due to a poorly mounted specimen. As a result, the modulus would then be determined from the linear region that is generated following the “toe” as the specimen “tightens up” in its initial stages of deformation [31].

3.4 Extrusion

Screw extrusion is probably the most important unit operation in polymer processing, in terms of its wide usage, and also its direct bearing on productivity and product quality. Most polymer products are extruded two times by screw extruders: the first time to make the polymer pellets by the material manufactures, and the second time to make the final products from the pellets. Screw extrusion often performs other functions in addition to melting, such a mixing, and chemical reaction [32].

The most frequently used extruder is a plasticating extruder, which is shown in Figure 15 [33].

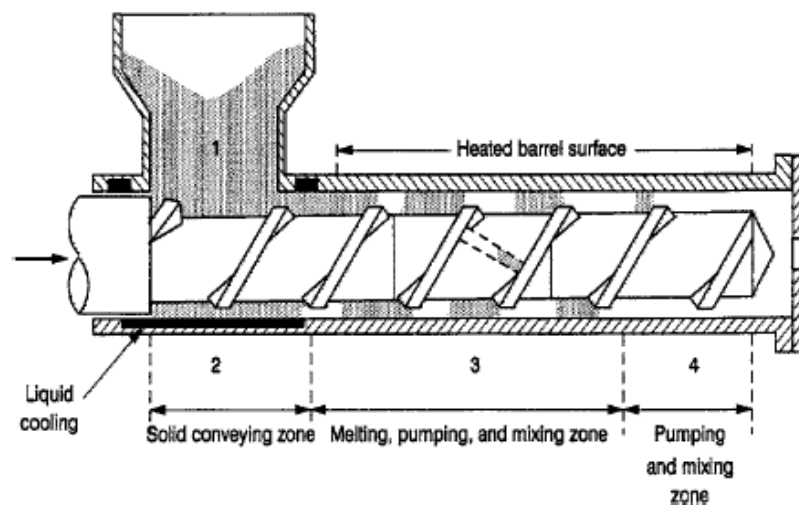


Figure 15. Single-screw plasticating extruder showing the four primary zones: hopper, solids feed, melting, and pumping [33]

Material enters from the feed hopper. Generally, the feed material flows by gravity from the feed hopper down into the extruder barrel. Some materials do not flow easily in dry form and special measures have to be taken to prevent hang-up (bridging) of the material in the feed hopper. As material falls down into the extruder barrel, it is situated in the annular space between the extruder screw and barrel, and is further bounded

by the passive and active flanks of the screw flight: the screw channel. The barrel is stationary and the screw is rotating. As a result, frictional forces will act on the material, both on the barrel as well as on the screw surface. These frictional forces are responsible for the forward transport of the material, at least as long the material is in the solid state (below its melting point) [34].

3.5 Compression molding

Compression molding is primarily used to process thermosetting systems and difficult to process thermoplastics, such as fiber-filled systems or thermoplastic elastomers. In the case of thermoplastics, a preheated mass of polymer, which may be either a sheet or a pile of pellets or powder, is placed in the mold. The temperature of the mold is set low enough to cause the polymer to solidify but not so rapidly that it will not flow. Hydraulic pressure is applied to the top or bottom plate pushing the plattens together. The molds are designed to prevent the top part of the mold from touching the bottom part, which would squeeze the material from the mold. The design of a compression molding process consists of four aspects. The first is the selection of the proper amount of material to fill the cavity when the mold halves are closed. The second is determining the minimum time required to heat the blank to the desired processing temperature and the selection of the appropriate heating technique (radiation heating, forced convection, etc.). It is necessary to make sure that the center reaches the desired processing temperature without the surface being held at too high of a temperature for too much time. The third is the prediction of the force required to fill the mold. Finally, the temperature of the mold must be determined, keeping in mind that one wants to cool the part down as rapidly as possible, but too rapid of a cooling rate will prevent the polymer from filling the mold [33].

II. EXPERIMENTAL BACKGROUND

4 MATERIALS

In this work, three commercially-available grades of PB-1 produced by Basell Polyolefins, Louvain la Neuve, Belgium were used. Typical properties of PB-1 grades are described in Table 4.

Table 4. Basic properties of PB-1 grades [35]

Typical properties		PB 8640M	DP 0401M	PB 0300M
Method				
Physical				
Density		0.906 g/cm ³	0.915 g/cm ³	0.915 g/cm ³
ISO 1183				
Melt flow index (190 °C / 2.16 kg)		1 g/10 min	15 g/10 min	4 g/10 min
ISO 1133				
Mechanical				
Flexural modulus		250 MPa	450 MPa	450 MPa
ISO 178				
Tensile strength at yield			22 MPa	19.5 MPa
ISO 8986-2				
Tensile strength at break		30 MPa	29 MPa	35 MPa
ISO 8986-2				
Tensile elongation at break		300 %	300 %	300 %
ISO 8986-2				
Melting temperature	T _{m1}	113 °C	126 °C	127 °C
DSC	T _{m2}	97 °C	114 °C	116 °C
These properties were measured in specimens conditioned for 10 days at 20 °C				

4.1 PB 0300M

Poly(1-butene) grade PB 0300M is a semi-crystalline homopolymer, which is used where creep, environmental stress crack resistance and elevated temperature performance are key requirements. This polymer is highly compatible with polypropylene due to its similar molecular structure. It is used to improve mechanical properties at elevated temperatures. It is less compatible in blends with polyethylene but it is still easily dispersible. It forms

a 2 phase structure which is the basis of the seal peel technology for easy-opening packaging applications.

It has relatively slow kinetics of crystallization which allows an excellent wetting behavior. Its highly shear-sensitive flow behavior means that it remains easily dispersible also in even more incompatible polymers like thermoplastic elastomers [35].

4.2 DP 0401M

Material DP 0401M is a semicrystalline homopolymer, which can be used where creep, environmental stress crack resistance and elevated temperature performance are key requirements. This polymer is highly compatible with polypropylene due to its similar molecular structure. It is less compatible in blends with polyethylene but it is still easily dispersible. Its relative slow crystallization kinetics allows for an excellent wetting behavior. Besides its high shear sensitive flow behavior, it remains easily dispersible, also in even more incompatible polymers like thermoplastic elastomers [35].

4.3 PB 8640M

Material PB 8640M is a random copolymer of butene-1 with low ethylene content. In blends with PE polymers, it forms a separate, but well-dispersed phase. Its primary use is as a minority blend component in the seal layer of easy-opening packaging films, produced by blown film extrusion. A typical PE blend partner for PB 8640M could be any ethylene homo- or copolymer in the melt index range of 0.5 to 2.0 g/10min.

Poly(1-butene) is also highly compatible with polypropylene due to its similar molecular structure, and it can be used to modify PP sealing behavior or mechanical properties such as impact strength. PB-1 crystallizes slowly and is very shear sensitive in its flow behavior [35].

5 SPECIMENS PREPARATION

5.1 Compression molding

Specimens designed for density measurement were prepared by compression molding from pellets of PB 0300M. Three plates (with dimensions of 12.5×12.5 mm) with various thickness 2, 1 and 0.5 mm were used. Plates were compression molded using hand-press at temperature of 170 °C for 5 minutes than cooled in hydraulic press at temperature of 60 °C for 10 minutes. Then, defined specimens were cut out from the sheet and they were stored at given temperature.

5.2 Extrusion

Extruder Brabender Plasti-Corder PLE 651 was used for extrusion of tapes from all grades of PB-1. The processing conditions were following for all materials: compression ratio of the screw 1:4; screw speed 20 rpm; barrel temperatures 135, 140, 145, 150 °C, extrusion slit die with profile 2×20 mm with temperature 150 °C.

5.3 Annealing

The prepared specimens were immediately after processing annealed at various temperatures: -22, 5, 22, 40 and 60 °C at atmospheric pressure for various times. The temperatures were chosen with respect to utilization of PB-1, which can be used for tanks, hose, tubing, molded parts, films, etc. at various temperatures. Two ovens (BinderBD23) with temperatures of 40 and 60 °C, refrigerator and freezer with common temperatures of 5 °C and -22 °C were employed for annealing of specimens. Temperature of 22 °C was in the laboratory room.

6 ANALYSING METHODS AND DEVICES

6.1 Density measurement

Densities of compression-molded specimens and extruded specimens were measured. Density measurement corresponds with the Standard ČSN 64 0111. The hydrostatic method was applied the principle of immersion method is determination of density in small plastic specimens. For this method a digital scale, KERN 770 (Figure 16) was used. As an immersion liquid, denatured ethanol was used and its density was measured by pycnometry.



*Figure 16. Digital scale
– KERN 770*

Compression-molded specimens were cut from sheets of different thicknesses (2, 1, 0.5 mm) to dimensions 35×20 mm. Each set of prepared specimens with three various thicknesses was annealed at given temperatures.

Dimensions of extruded specimens for density testing were 35×20 mm with thickness 2 mm. Specimens from each of material were stored in the same conditions as compression-molded specimens. The material DP 0401M was annealed only at temperatures of 22 °C, 22 °C and 60 °C.

6.2 Wide angle X-ray scattering

For scattering in the transmission mode, diffraction angle with interval $2\theta = 7 - 25^\circ$, the measuring step of 0.05° and holding time of 5 s were used. A URD6 diffractometer CuK α radiation monochromatized with a Ni filter ($\lambda = 0.154$ nm) was employed. Whole

extrudates of material PB 0300M with dimensions 2×20×50 mm were used as specimens for scattering.

The reflections relative to the tetragonal modification of PB-1 are basically three main peaks at 11.9, 16.9 and 18.48 2θ , corresponding to the (200), (220) and (301) planes. The hexagonal form I is characterized by four signals at 9.9, 17.3, 20.2 and 20.58 2θ , originated by the (110), (300), (220) and (211) planes, respectively [36]. It may be noted that, as a consequence of the phase transition, with increasing time the intensity of the peaks typical of the hexagonal form I (i.e.(110) at 9.98 2θ) increases, whereas the intensity of peaks related to the tetragonal form II (i.e. (200) at 11.98 2θ) decreases.

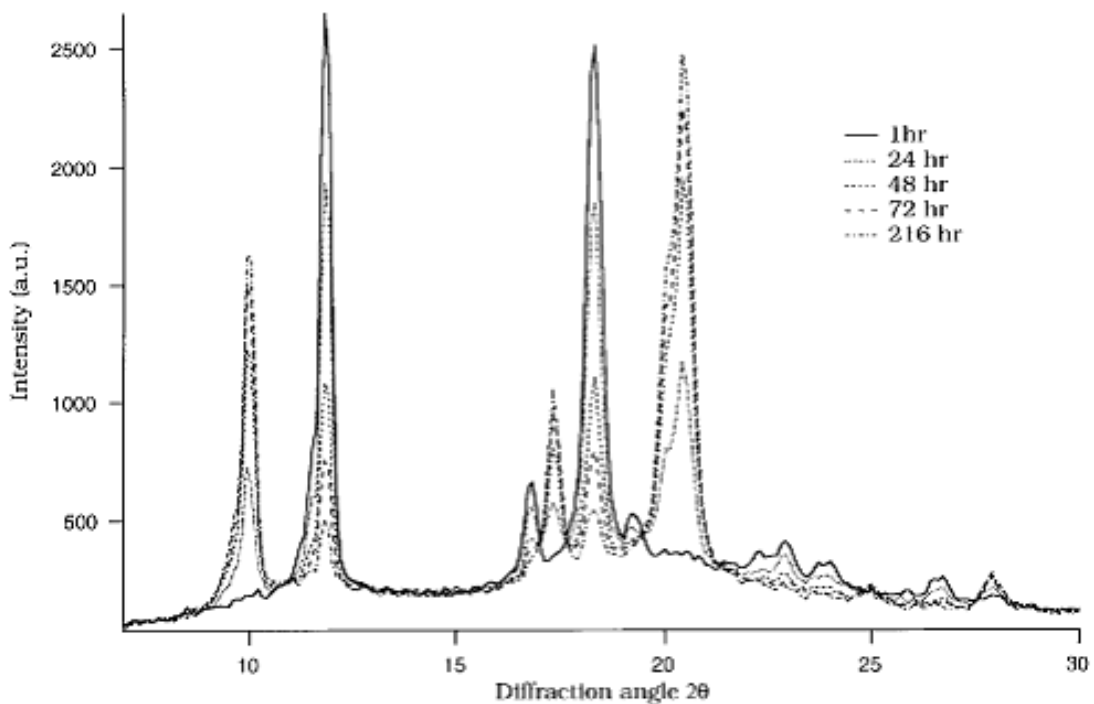


Figure 17. Wide angle X-ray scattering patterns at different times [15]

The PeakFit v4 was used for the evaluation of crystalline part in the specimens. Furthermore, the content of the forms I and II during phase transformation was calculated by following the modified study of Marigo et al. [15]. It is suggested to follow the disappearing of the peak at 11.8° 2θ (reflection plane 200) the form II rather than increase the peak at 9.9° 2θ (reflection plane 110) of the form I (see Figure 17) because, together with the phase transformation, a post crystallization phenomenon takes place during which part of the amorphous polymer crystallizes into the form I. However, in this

work, it was not possible to measure the identical specimen but a series of specimens prepared under controlled conditions. It was decided to follow evolution of the both peaks of the forms I and II (at 9.9° and $10.8^\circ 2\theta$) and calculate the ratio of heights the peaks and content of the form I from the total sum of both heights. The same approach has been used in several works by Azzuri et al. [37], Samon et al. [38] and Natta et al. [39]. The similar approach was used in work of Kaszonyiova et al. [40] or in case of isotactic polypropylene, which is also a polymorphic material [41, 42].

6.3 Tensile testing

Mechanical properties, tensile properties of the specimens were measured by a Zwick 145665 tensile tester. The tensile characteristics were evaluated by tester internal software TestXpert V7.11. Five specimens (average values are reported) from each material for each temperature were tested with constant speed 100 mm/min. Yield stress, stress at break and elongation at break were derived from the stress/strain traces. Besides, the elastic modulus was evaluated using a Zwick external extensometer (gauge length of 20 mm) at a test speed of 1mm/min.

Specimens from each of material were measured during annealing time of 86 days. Five specimens of each material and all five temperatures were tested. Specimens were cut out the long tape after cooling. Dimensions of these specimens were length 160 mm, width 20 mm, and thickness 2 mm.

Consequently, specimens from PB 0300M and PB 8640M were annealed to the five different temperature places -22 , 5 , 22 , 40 and 60 °C. DP 0401M was exhibited to -22 °C, 60 °C and 22 °C.

III. RESULTS AND DISCUSSION

7 DENSITY MEASUREMENT

7.1 Evolution of density of extrudates

In following three figures (18 – 20) it can be seen that densities of extrudates increase with rising annealing time in all grades of PB-1 at all annealing temperatures except -22 and 60 °C in PB 8640M. It can be seen that the fastest evolution occurs at temperatures of 5 and 22 °C in all materials. The increase at annealing temperature of 40 °C led to a slight decrease of evolution and further increase to 60 °C slows down the phase transformation. This is more pronounced in copolymer PB 8640M, which has the lowest crystallization temperature [43] and thus competition between secondary crystallization and the phase transformation II – I occurs. The transformation behavior at temperature of -22 °C is not completed during initial seven days and it follows the findings from previous research of Beníček et al. [14, 43].

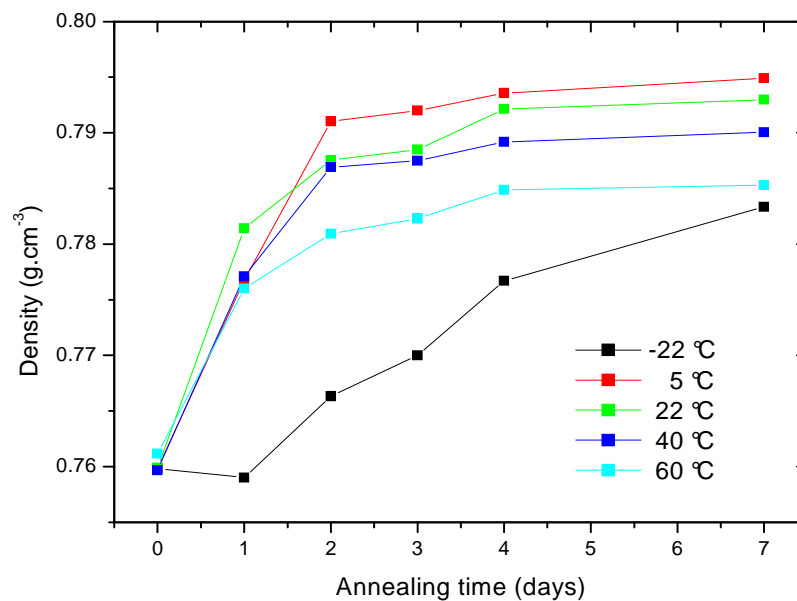


Figure 18. PB 0300M – evolution of density in extrudates

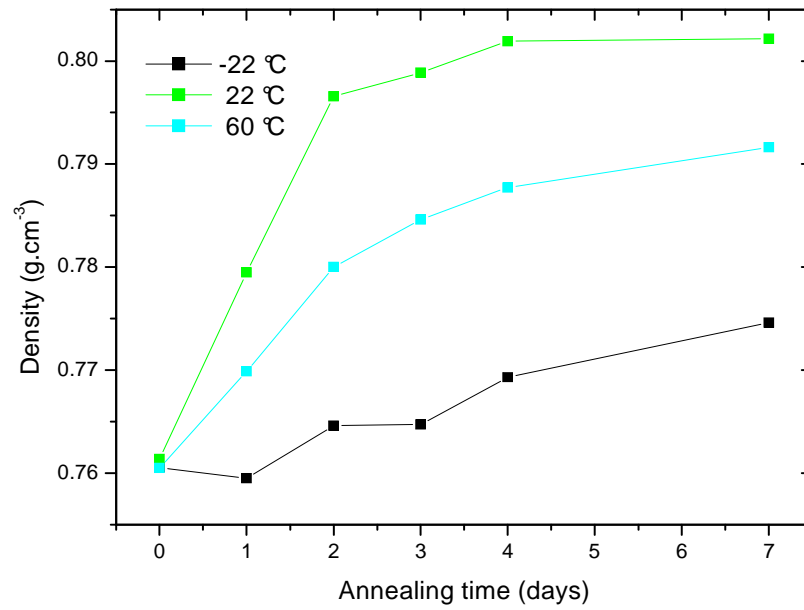


Figure 19. DP 0401M – evolution of density in extrudates

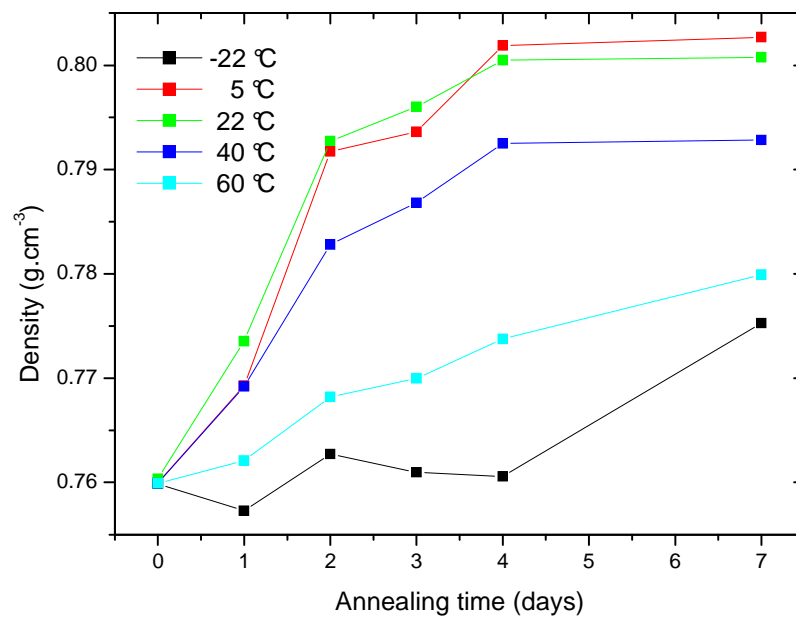


Figure 20. PB 8640M – evolution of density in extrudates

7.2 Evolution of density of compression-molded specimens

The density evolution of compression-molded specimens from material PB 0300M is illustrated in Figures 21 – 23. Again, increasing trend in evolution is observed and it is virtually the same evolution as could be seen in the extrudates (Figure 18). Different values of density show specimens annealed at -22 °C for all three thicknesses of the compression-molded specimens in comparison with the extrudates.

It can be seen that the different thicknesses of compression-molded specimens does not influence the evolution of the density in compression-molded specimens respectively the rate of the phase transformation.

It should be noted that measured densities differs from table values (Table 2) of individual forms of PB-1 and from datasheet's values [8, 35]. Nevertheless, densities of compression-molded and extrudates are virtually the same after the transformation. Probably, further measurement of density during the phase transformation would be desirable on specimens prepared under various crystallization conditions.

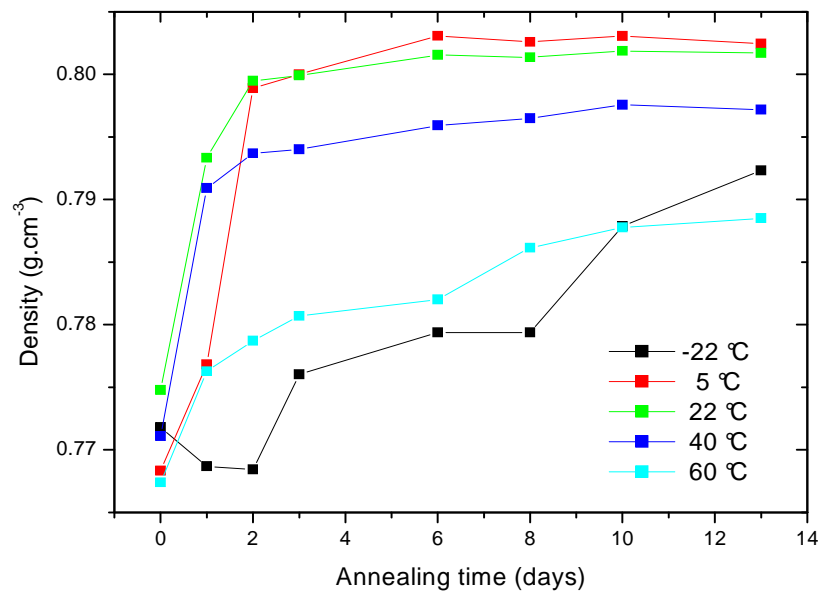


Figure 21. Evolution of density in compression-molded specimens with thickness of 0.5 mm

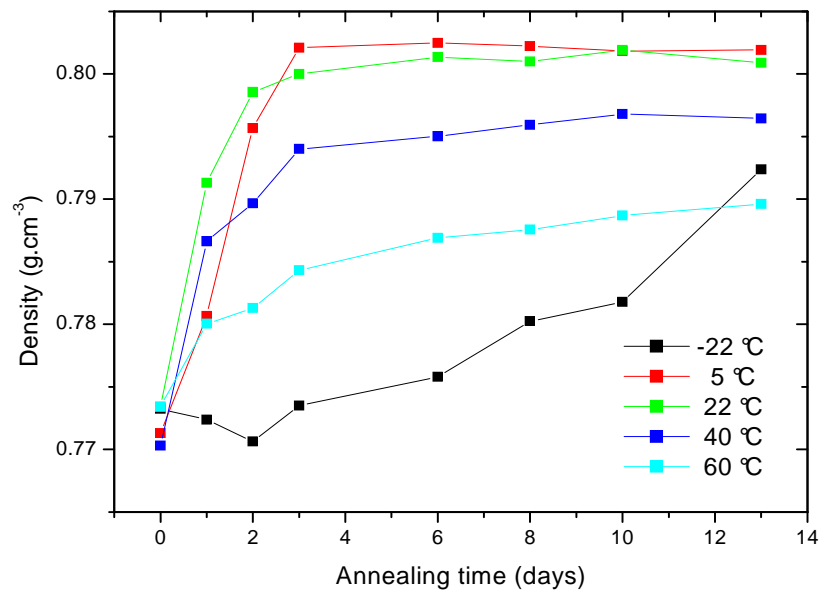


Figure 22. Evolution of density in compression-molded specimens with thickness of 1 mm

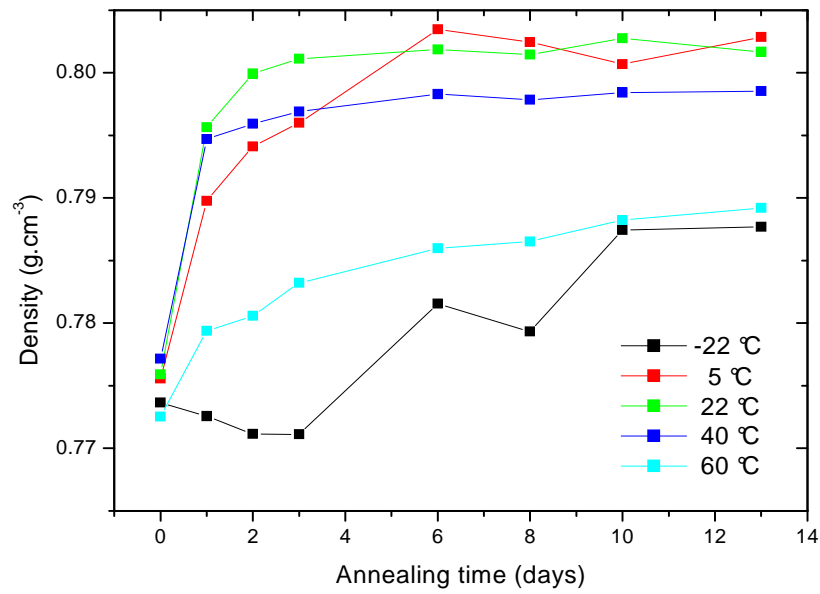


Figure 23. Evolution of density in compression-molded specimens with thickness of 2 mm

8 WIDE ANGLE X-RAY SCATTERING

As can be seen in Figure 24, the content of the form I increases with increasing annealing time. During initial five days, the fastest increase of the form I was observed at temperatures of 5 °C and 22 °C. This observation follows those from density measurements. A specific behavior shows only specimen annealed at -22 °C with gradual increase of form I content during initial fifteen days, followed by rapid increase to the values between annealing temperatures of 40 and 22 °C.

When evolution at temperature of 60 °C is compared with density evolution (Figure 18), one would expect higher content of form I. Nevertheless, this observation is confirmed in following chapter 9 Tensile testing. This finding opens a question whether a critical minimum content of form I accelerates the rate of the phase transformation at low annealing temperature of -22 °C.

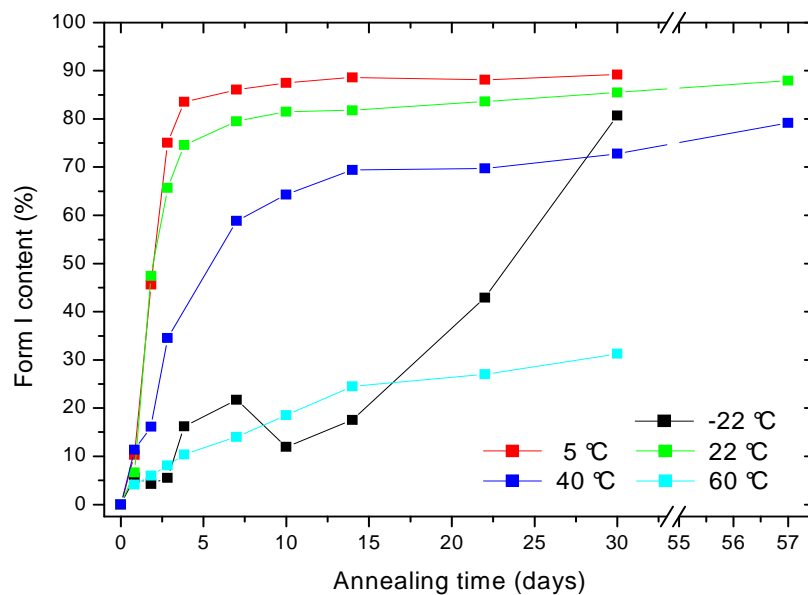


Figure 24. PB 0300M – evolution of form I content

9 TENSILE TESTING

Tensile testing was performed in order to observe the evolution of tensile properties during the phase transformation in extrudates, which are commonly processed from PB-1. As was observed in study of Beníček et al. [14] with injection molded specimens, tensile modulus and tensile strength at break increase during the phase transformation in dependence on annealing temperature.

They studied [14] the thermal-induced transformation of injection-molded PB-1. The same grades of PB-1 (PB 0300M, DP 0401M, and PB 8640M) were used. These specimens were also annealed at the same temperatures of -22, 5, 22, 40, and 60 °C for annealing time of 0 – 48 days.

9.1 Evolution of tensile modulus

The evolution of tensile modulus is illustrated in Figures 25 – 27. It was observed in all materials that tensile moduli increase with increasing annealing time. During initial seven days the increase of moduli is remarkable, especially at annealing temperatures of 5 °C and 22 °C. For these specimens plateau is achieved from the thirtieth day.

For temperature of 60 °C the situation is completely different. In case of homopolymers (PB 0300M and DP 0401M) fast growth of moduli is not observed during initial five days. After this time, moduli slowly increase and from the day thirteen the plateau can be seen. A similar behavior was observed in specimens annealed at temperature of -22 °C where the increase is slower, but after a distinct time a rapid increase can be seen, which results to stable moduli between values of specimens annealed at 22 and 40 °C in all materials.

When tensile modulus of material PB 0300M (Figure 25) is compared to the form I content calculated from WAXS (Figure 24) it can be seen that the trends are practically the same. Thus, the suggestion with a minimal critical amount of the form I seems to be relevant. Also, the evolution of the phase transformation measured from the evolution of tensile modulus is a suitable method. The comparison with density measurements is limited, nevertheless the main trends are observed as well.

Values of moduli in homopolymers are significantly higher than for ethylene copolymer (PB 8640M). Generally PB-1 possesses higher tensile modulus than polyethylene and as a result of copolymerization a lower modulus is expected. This material also transforms more readily than homopolymers as was observed in recent studies [14, 43].

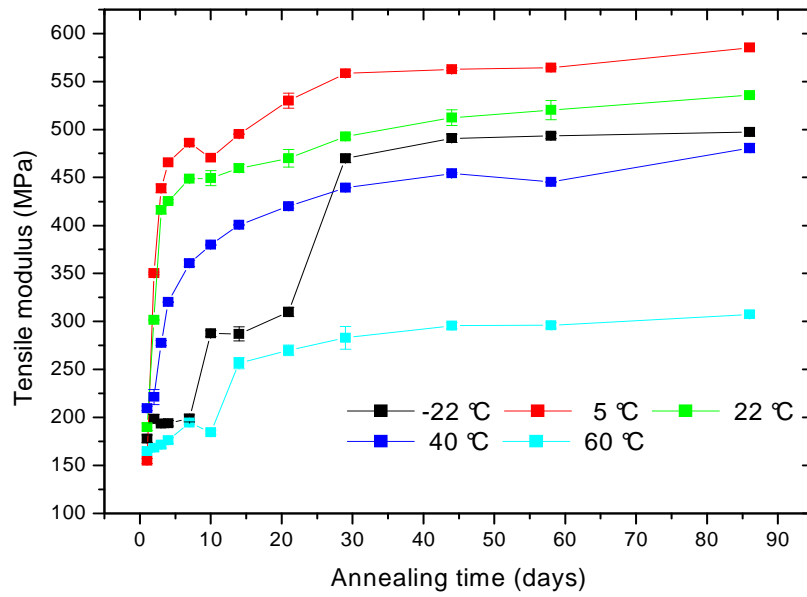


Figure 25. PB 0300M – evolution of tensile modulus in extrudates

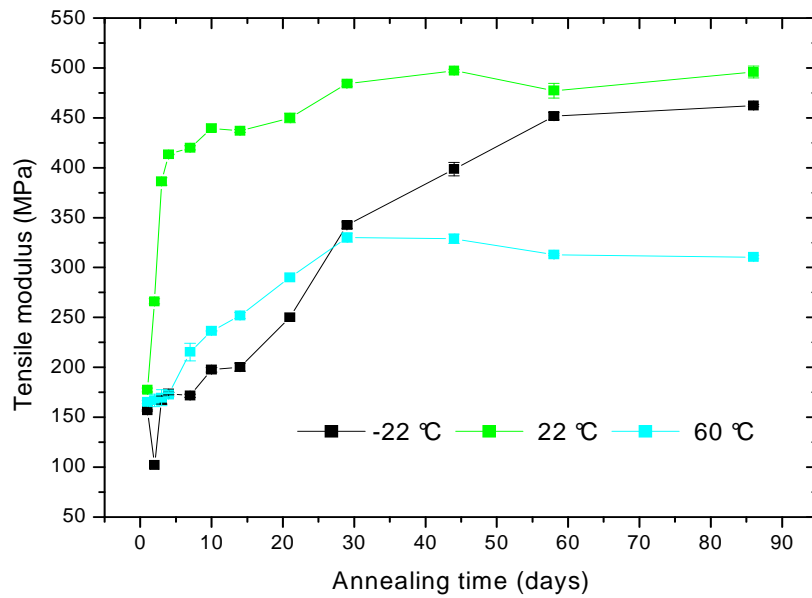


Figure 26. DP 0401M – evolution of tensile modulus in extrudates

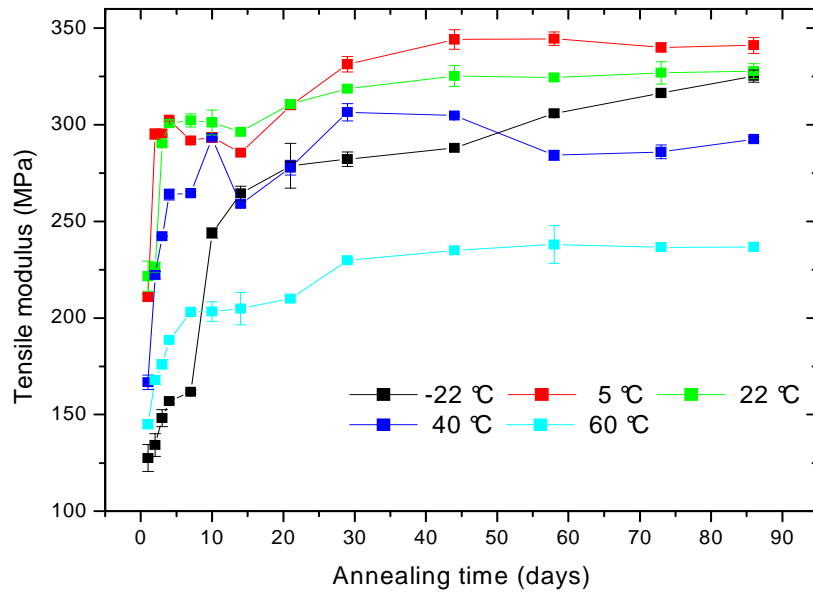


Figure 27. PB 8640M – evolution of tensile modulus in extrudates

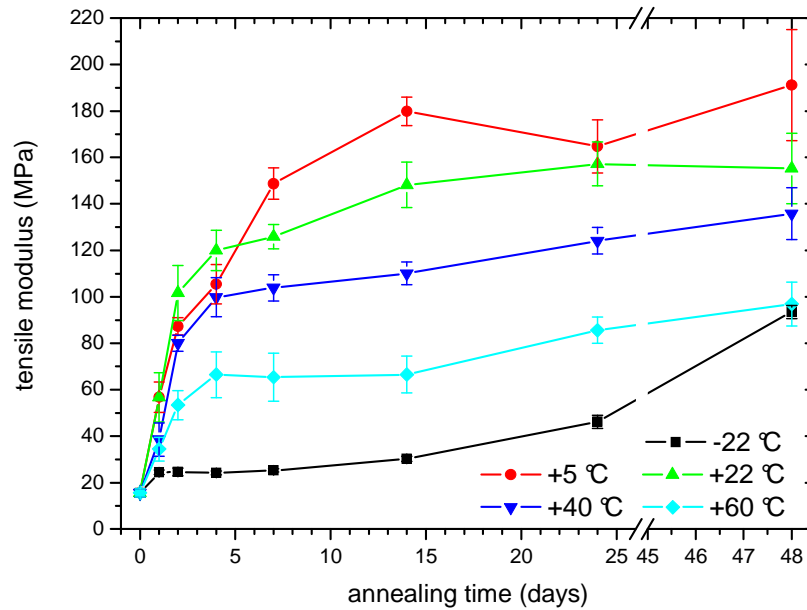


Figure 28. Evolution of tensile modulus in injection-molded PB 0300M [43]

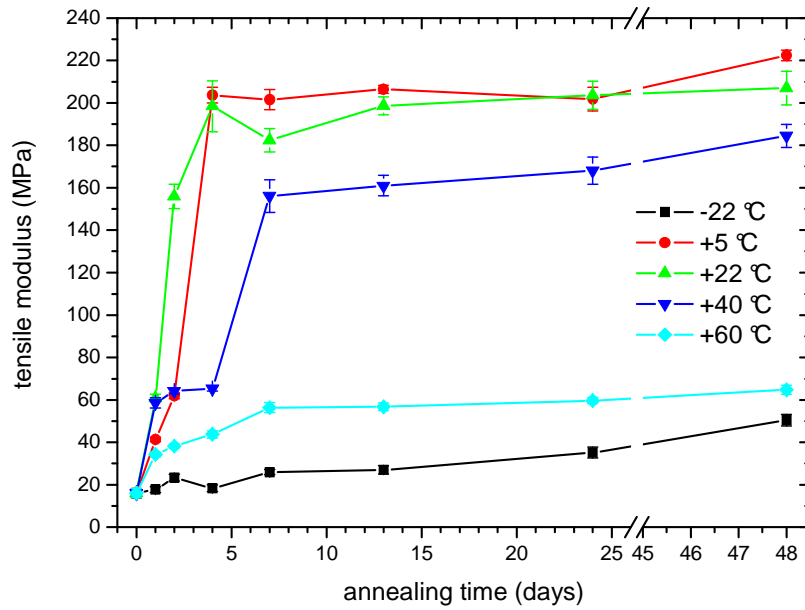


Figure 29. Evolution of tensile modulus in injection-molded DP 0401M [43]

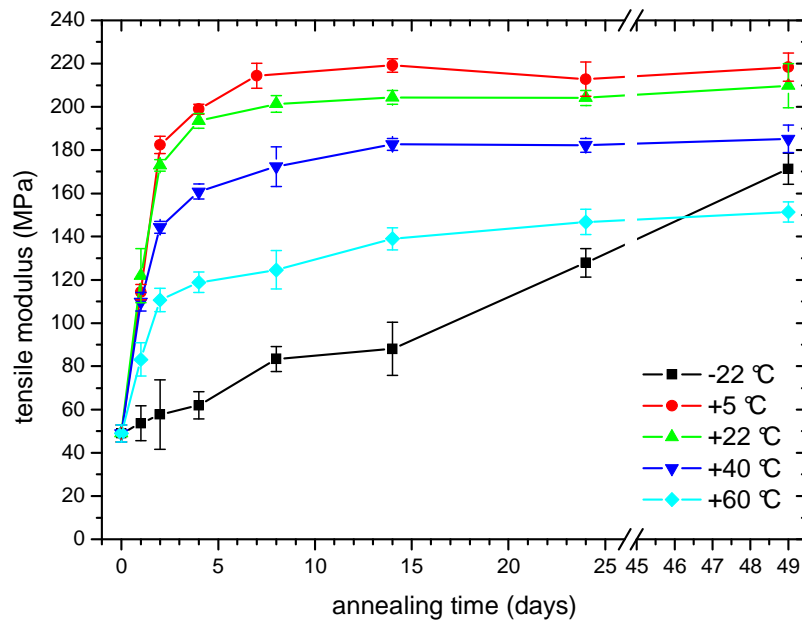


Figure 30. Evolution of tensile modulus in injection-molded PB 8640M [43]

Beníček et al. [14] found that the non-monotonic evolution of tensile modulus in dependence on annealing temperature is obvious. In all materials, the fastest evolution is evident at temperature of 6 and 22 °C, followed by a bit slower evolution at temperature of 40 °C. At annealing temperatures of -22 and 60 °C slow evolution was observed without

rapid increase at $-22\text{ }^{\circ}\text{C}$. As written above, copolymer PB 8640M possesses higher transformation rate and thus at annealing temperature $-22\text{ }^{\circ}\text{C}$ an increase of modulus is observed – remarkably later than in extrudates.

Further important remark is that values of moduli in extrudates are remarkably higher than in injection-molded specimens (Figures 28 – 30). The morphology of extrudates possesses only spherulitic structure [43] while in injection-molded specimens a typical skin-core morphological structure is achieved.

These findings show a significant influence of processing on the rate of the phase transformation in PB-1.

9.2 Evolution of tensile yield strength

It was observed in all PB-1 materials (Figure 31 – 33) that tensile yield strength increases with annealing time. Nevertheless, the observation of yield strength seems to be depending on material properties (molecular weight), annealing temperature and a minimum the form I content. In (Figure 33) copolymer (PB 8640M) is observed fast increase during initial five days of tensile yield strength for temperatures of 5 and 22 °C. After this time, yield strengths slowly increase and the plateau is reached from the day thirty. On the other hand, in both homopolymers (Figure 31 and 32) observation of yield strength is limited to low annealing temperatures of -22 and 5 °C and not from day 0.

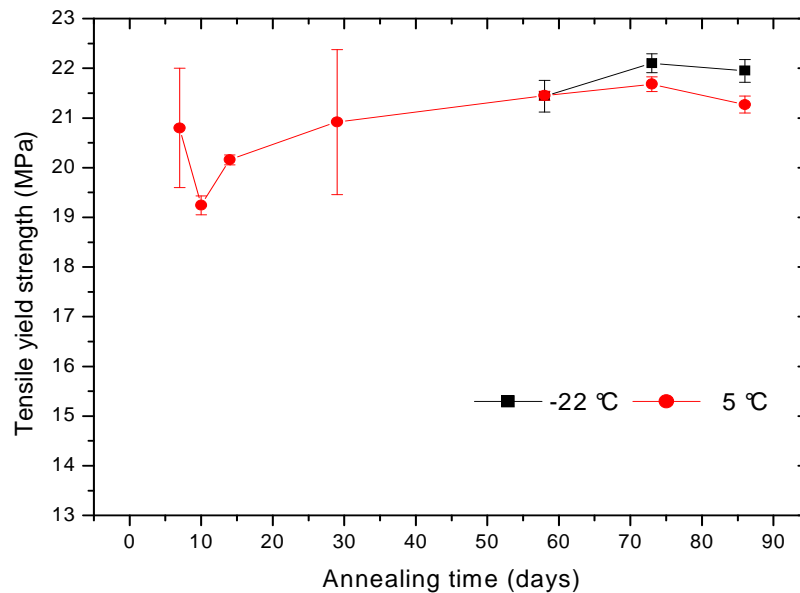


Figure 31. PB 0300M – evolution of tensile yield strength in extrudates

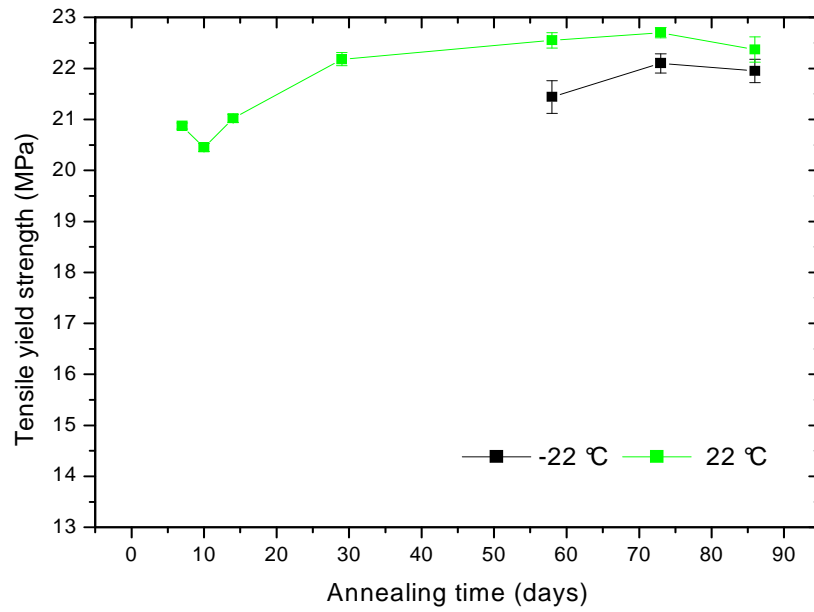


Figure 32. DP 0401M – evolution of tensile yield strength in extrudates

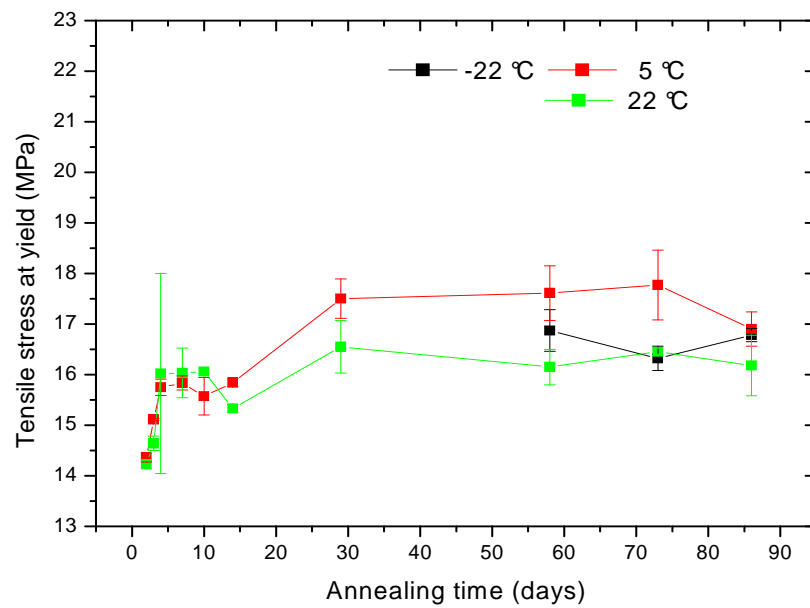


Figure 33. PB 8640M – evolution of tensile yield strength in extrudates

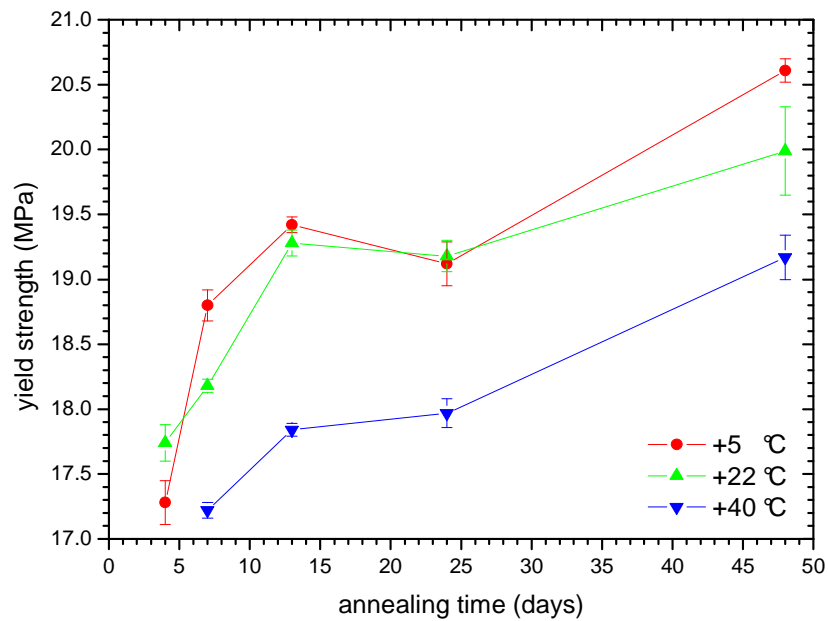


Figure 34. Evolution of tensile strength at yield
in injection-molded DP 0401M [43]

When evolution of yield strength of extruded (Figure 32) and injection-molded (Figure 34) DP 0401M are compared a significant difference can be seen. Yield strength was observed in extrudates at temperature of 5 °C and partly at -22 °C but in injection molded it was between temperatures of 5 ~ 40 °C. From this observation it is evident that processing is a key parameter influencing mechanical properties and also the rate of the phase transformation.

9.3 Evolution of tensile strength at break

The evolution of tensile strength at break is illustrated in Figures 35 – 37. It can be seen that tensile strength at break decreases with increasing annealing time in all materials. Minimum values are observed after thirty days in case of both homopolymers (DP 0401M and PB 0300M). The evolution in copolymer PB 8640M is remarkably different where values vary. Again, the fastest evolution was observed at annealing temperature of 5 and 22 °C in all materials.

When evolutions of extrudates and injection-molded specimens (Figure 38) from PB 0300M are compared the opposite trend can be seen. Evolution of tensile strength at break in injection-molded specimens gradually rises with increasing annealing time as can be seen in Figure 38, while evolution of tensile strength at break in extrudates decreases with increasing annealing time as can be seen in Figures 35 – 37. It can be seen in case of PB 0300M that values from both sets of specimens converge to a plateau with the virtually same value.

This is further evidence of influence of processing conditions on evolution of mechanical properties of PB-1.

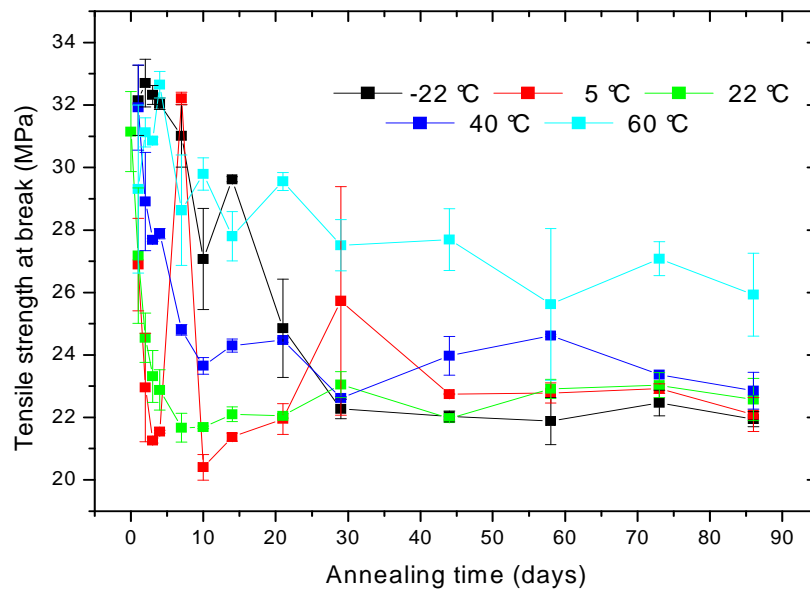


Figure 35. PB 0300M evolution of tensile strength at break in extrudates

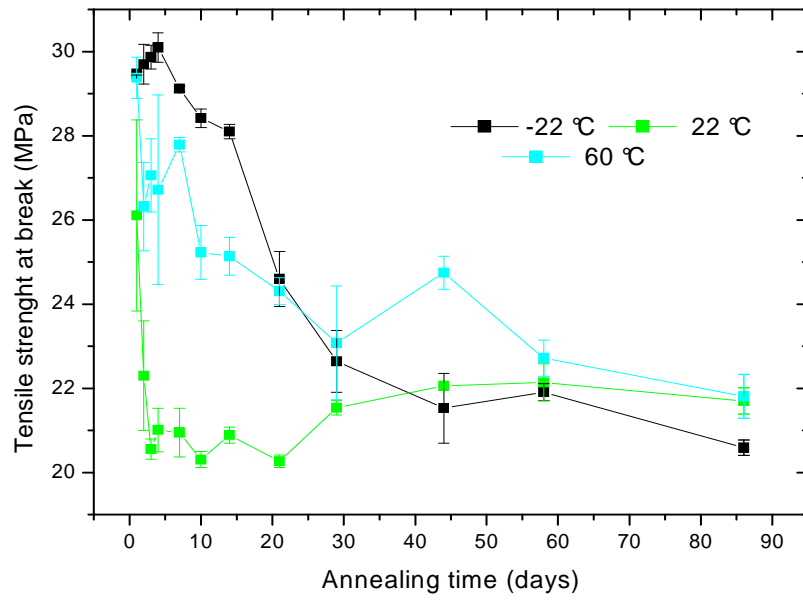


Figure 36. DP 0401M – evolution of tensile strength at break in extrudates

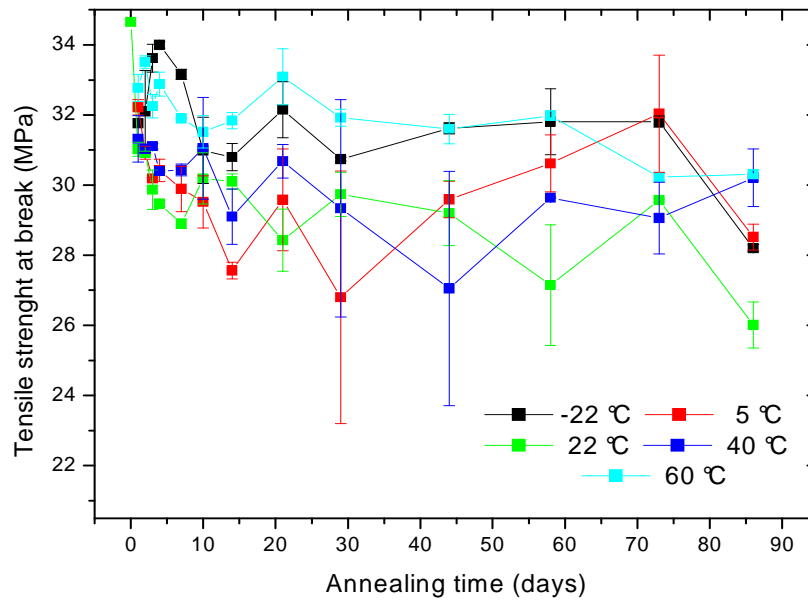


Figure 37. PB 8640M – evolution of tensile strength at break in extrudates

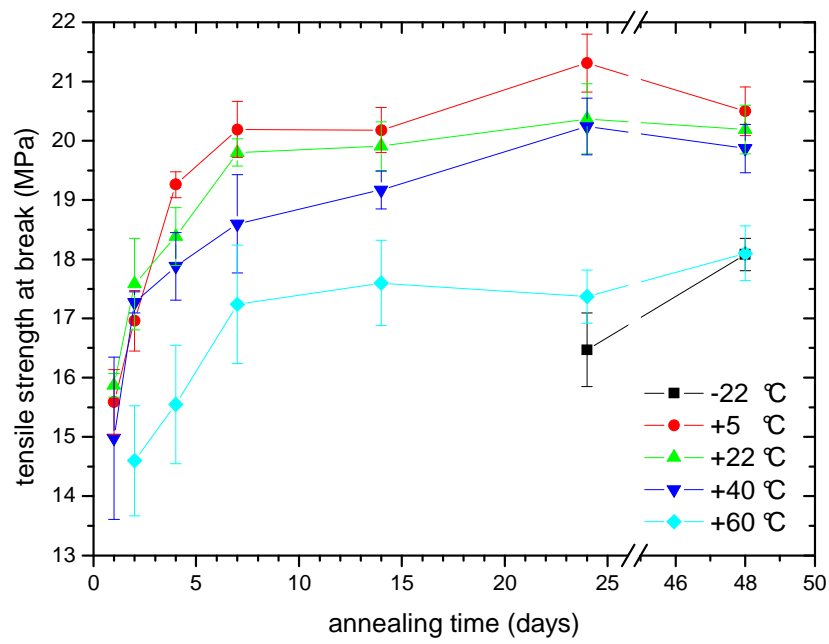


Figure 38. Evolution of tensile strength at break
in injection-molded PB 0300M [43]

9.4 Evolution of tensile elongation at break

As can be seen in Figures 39 – 41 tensile elongations at break decrease with increasing annealing time in all materials. The same trend was also observed in study of Benicek et al. [14]. It is an opposite effect to the evolution of tensile modulus. In both homopolymers (Figures 39 and 40) significant decrease of elongation at break with increasing annealing time can be seen. On the other hand in copolymer PB 8640M (Figure 41) the evolution shows variation of values.

Again, when extrudates compared with injection-molded specimens of PB 0300M significant difference is obvious in drawability, which is surprisingly higher in extrudates even if one would suppose higher drawability of oriented injection-molded specimens.

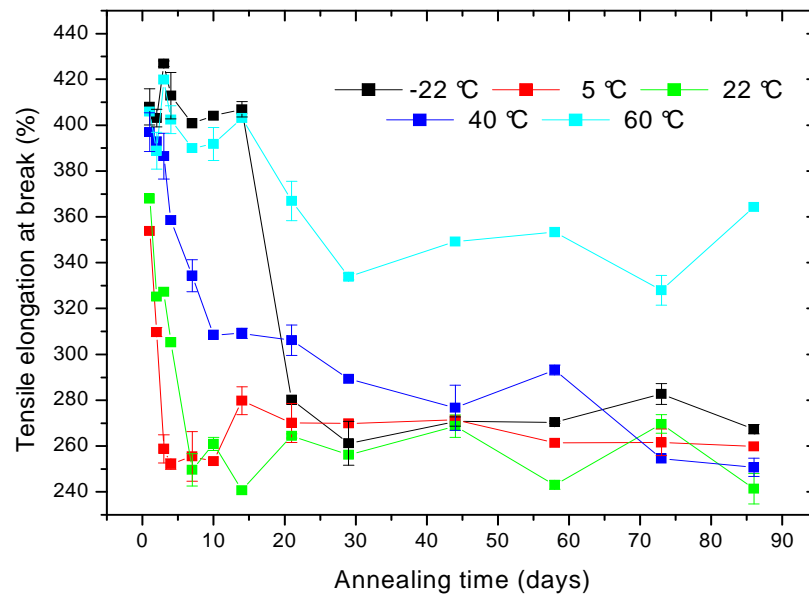


Figure 39. PB 0300M – evolution of tensile elongation at break in extrudates

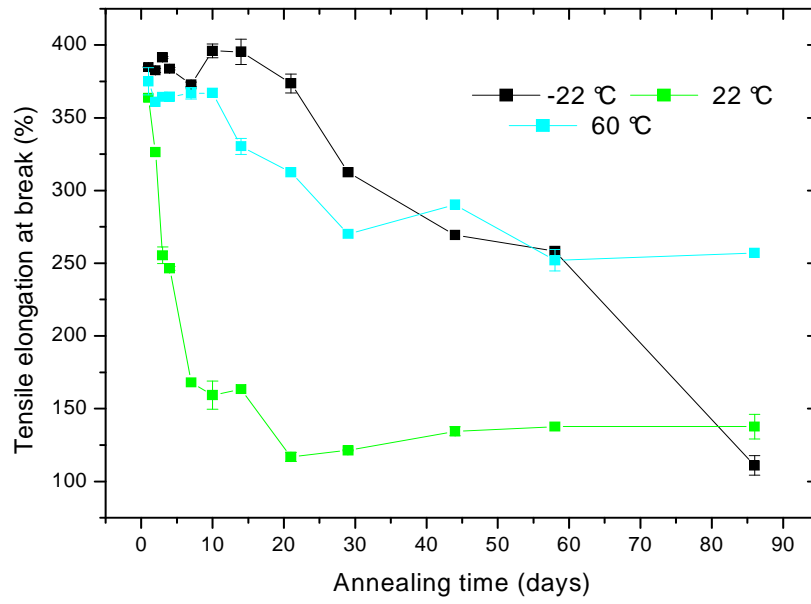


Figure 40. DP 0401M – evolution of tensile elongation at break in extrudates

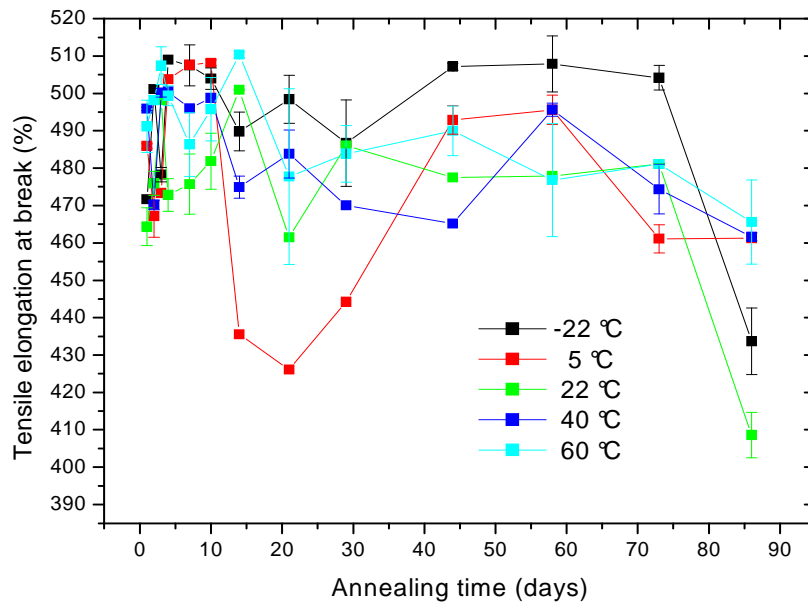


Figure 41. PB 8640M – evolution of tensile elongation at break in extrudates

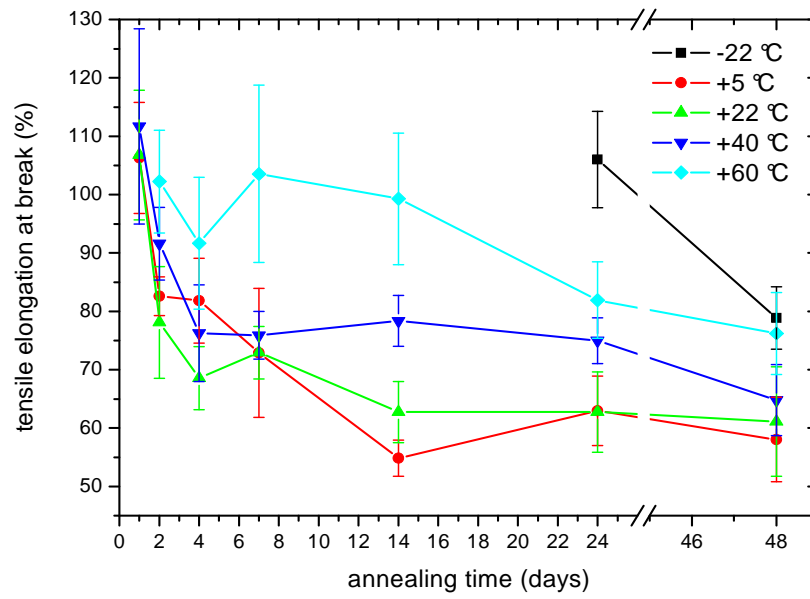


Figure 42. Evolution of tensile elongation at break in injection-molded PB 0300M [43]

CONCLUSION

This Master thesis deals with the evolution of physical and mechanical properties during the phase transformation from the metastable form II into the thermodynamically stable form I in PB-1. In the beginning, present knowledge concerning the phase transformation is introduced. The experimental part has been divided to density measurement and tensile testing, then the results are discussed and compared with previous study of the phase transformation of PB-1.

From the results of density measurements, it is obvious that the different thicknesses of compression-molded specimens do not influence the evolution of rate of the phase transformation. Densities of compression-molded and extrudates possess virtually the same values after the phase transformation. In both cases, the fastest transformation rate was observed at annealing temperatures of 5 and 22 °C. At higher or lower temperature (60 and -22 °C) the transformation rate decreases with distinct differences.

Then, the extrudates were analyzed by wide angle X-ray scattering and the content of the form I was calculated. Thus, the calculated evolution follows the trends, which were observed, via density measurements. Furthermore, this evolution of the form I content was confirmed by tensile testing in the evolution of tensile modulus. This finding opens a question whether a critical minimum content of the form I accelerates the rate of the phase transformation at the lowest annealing temperature.

The study of evolution of the tensile properties was carried out on extrudates and the results were consequently compared with the evolution of injection-molded specimens. From this observation, it was found that values of moduli in extrudates are remarkably higher than in the injection-molded specimens. This is a consequence of different morphological structures, which have direct impact on mechanical properties and the phase transformation in PB-1. Further, from the observation of yield strength a dependence on material properties (molecular weight), annealing temperature and a minimum form I content seems to be relevant. When tensile strengths at break were compared, opposite trend in evolution was observed. While in extrudates strength at break decreased with increasing annealing time, in injection-molded specimens increased. Nevertheless, values of the both evolutions converged to the equilibrium value of tensile strength.

In the evolution of tensile elongation at break, surprising findings could be seen. One would expect higher drawability in oriented injection-molded, however, remarkably higher drawability was observed in extrudates.

From these observations and comparisons of tensile characteristics, it is evident that processing is a key parameter influencing mechanical properties and together with annealing temperature significantly influence the rate of the phase transformation of PB-1.

REFERENCES

- [1] **Brydson, J.** *Plastics Materials*. 7th ed., *Elsevier*, 1999, ISBN 978-0-7506-4132-6.
- [2] **Plastics Design Library Staff.** *Handbook of Plastics Joining*. *William Andrew Publishing/Plastics Design Library*, 1997, ISBN 978-1-884207-17-4.
- [3] **White, J.L. and Choi, D.D.** *Polyolefins – Processing, Structure Development, and Properties*. *Hanser Publishers*, 2005, ISBN 978-1-56990-369-8.
- [4] **Oxford paperback references.** *A Dictionary of Science*. 5th ed., *New York, OXFORD University press*, 2005, ISBN 978-0-19-280641-3.
- [5] **Nakamura, K., Kanamoto, T., et al.** *Macromolecules*. 1999, Vol. 32, p. 4975.
- [6] **Kalay, G. and Kalay, C.R.** *J. Appl. Polym. Sci.* 2003, Vol. 88, p. 714.
- [7] **Schemm, F., Vliet, F., Könnecke, K., Grasmeyer, J.** *Polybutene-1: entering the next generation*. [online]. © 2005, [cit. 2009–3–16].
< <http://www.pbpsa.com/eng/downloads/conf-plasticpipes2004.pdf> >.
- [8] *Polybutene-1: pipe extrusion guide*. s.l. *Basell Polyolefine*, 2005.
- [9] **Maring, D., et al.** *J. Polym. Sci.* 2000, Vol. 38, p. 2611.
- [10] **Huang, Q., et al.** *Polym. Int.* 2001, Vol. 50, p. 45.
- [11] **Huang, Q.G. et al.** *Chinese Chemical Letters*, 2007, Vol. 18, p. 217.
- [12] **Kozłowska, M.K., et al.** *Journal of Chromatography A*. 2005, Vol. 1068, p. 297.
- [13] **DiLorenzo, M.L., Righetti, M.C.** *Polymer*. 2008, Vol. 49, p. 1323.
- [14] **Beníček, L., Chvátalová, L., Čermák, R., Verney, V.** *ANTEC 2008-Society of Plastic Engineers, Milwaukee, WI, USA*, 2008.
- [15] **Marigo, A., Marega, C., Ferrara, G., et al.** *Europ. Pol. J.* 2000, Vol. 36, p. 131.
- [16] **Choi, C., White, J.L.** *Polymer Engineering and Science*. 2001, Vol. 41, p. 933.
- [17] **Winkel, A.K., Miles, M.J.** *Polymer*. 2001, Vol. 41, p. 2313.
- [18] **Yan, S., Jiang, S., Duan, Y., et al.** *Polymer*. 2004, Vol. 45, p. 6365.
- [19] **Grizzuti, N., Coppola, S., Balzano, L., et al.** *Polymer*. 2004, Vol. 45, p. 3249.

- [20] **Winter, H.H., Grizzuti, N. and Acierno, S.** *Macromolecules*. 2002, Vol. 35, p. 5043.
- [21] **Samon, J.M., Schultz, J.M., Hsiao, B.S.** *Macromolecules*. 2001, Vol. 34, p. 2008.
- [22] **Brandrup, J., Immergut, E.H. and Grullke, E.A.** *Polymer handbook*. 4th.ed., 1999, ISBN 0-471-16628-6.
- [23] **Basell Polyolefins.** Polybutene-1 [online]. © 2008, [cit. 2009–04–23].
< <http://www.bpf.co.uk/Plastipedia/Polymers/Polybutene1.aspx> >.
- [24] **Potter, T.** Mass Density [online]. © 2005, [cit. 2009–04–22].
< <http://www.tompotter.us/massdensity.html> >.
- [25] **Český normalizační institut, Praha.** ČSN 64 0111. *Brno, s. p. Print*, 1993.
- [26] **Wikipedia.** Wide Angle X-ray Diffraction [online]. 2009–05–04, [cit. 2009–05–05]. < http://en.wikipedia.org/wiki/Wide_angle_X-ray_scattering >.
- [27] **Roe, R. J.** *Methods of X-ray and neutron scattering in polymer science*. Oxford University press, Inc., 2000, ISBN 0-19-511321-7.
- [28] **Mirau, P.A., Bovey, F.A., Jelinski, L.W.** *Macromolecules, Structure in Encyclopedia of physical science and technology*. Elsevier, 2001.
- [29] **University of California, Santa Barbara.** X-ray Generation & Properties [online]. © 2007, [cit. 2009–04–23].
< <http://www.mrl.ucsb.edu/mrl/centralfacilities/xray/xray-basics/index.html#TOP> >.
- [30] **University of Cambridge.** X-ray Diffraction [online]. © 2002, [cit. 2009–04–23].
- [31] **Wilkes, G.L.** *Polymers, mechanical behavior in Encyclopedia of physical science and technology*. Elsevier, 2001.
- [32] **Chung, CH.I.** *Extrusion of Polymers Theory and practice*. Carl Hanser Verlag, Munich, 2000. ISBN 3-446-21376-7.
- [33] **Baird, D.G. and Collias, D.I.** *Polymers processing*. John Wiley & Sons, New York, 1998. ISBN 0-471-25453-3.
- [34] **Rauwendaal, CH.** *Polymer Extrusion*. Carl Hanser Verlag, Munich, 2001. ISBN 3-446-21774-6.

- [35] **LyondellBasell.** Polybutene-1 [online]. © 2008, [cit. 2009-04-25].
<http://www.basell.com/portal/site/basell/menuitem.81bd1022b7c8ec5bbaabbd10e5548a0c/?VCMChannelID=9a76746516cf4110VgnVCM100000646f3c14____&productQueryText=&filterType=resin&resin=2&market=®ion>.
- [36] **Lauritzen, J. I., Jr. and Hoffman, J. D. J.** *Appl. Phys.* 1973, Vol. 44, p. 4340.
- [37] **Azzuri, F., et al.** *Macromolecules.* 2004, Vol. 37, p. 3755.
- [38] **Samon, J.M., et al.** *J. Polym. Sci., Part B: Polym. Phys.* 2000, Vol. 38, p. 1872.
- [39] **Natta, G., Corradini, P. and Bassi, I.** *Nuovo Cimento Suppl.* 1960, Vol. 15, p. 52.
- [40] **Kaszonyiová, M., Rybníkář, F. and Geil, P.H.** *J. Macromol. Sci. Phys.* 2004, Vol. 43, p. 1095.
<http://www-outreach.phy.cam.ac.uk/camphy/xraydiffraction/xraydiffraction_index.htm>.
- [41] **Obadal, M., Čermák, R. and Stoklasa, K.** *Macromol. Rapid. Commun.* 2005, Vol. 26, p. 1253.
- [42] **Turner-Jones, A., Aizlewood, J.M., Beckett, D.R.** *Macromol. Chem.* 1964, Vol. 74, p. 134.
- [43] **Beníček, L.** Doctoral thesis, *Universite Blaise Pascal, Clermont-Ferrand, France*, 2009.

LIST OF SYMBOLS

Å	Angström
AFM	Atomic force microscopy
DSC	Differential scanning calorimetry
E	Young's modulus
FIC	Flow index crystallization
ISO	International organization for standardization
MW	Molecular weight
MWD	Molecular weight distribution
n	Index of refraction
NMR	Nuclear magnetic resonance
PB-1	Isotactic poly(1-butene)
ppm	Parts per million
rpm	Rotations per minute
RT	Room temperature
SAXS	Small angle X-ray scattering
T_d	Draw temperature
T_m	Melting temperature
WAXS	Wide angle X-ray scattering
γ	Crystal lattice parameter [°]
ε_b	Elongation at break
ε_y	Elongation [%]
θ	Bragg angle [°]
λ	Wave length
σ_b	Stress at break

σ_y	Stress at yield
ψ	Rotation angle [°]

LIST OF FIGURES

Figure 1. Structure of various polyolefins [7].....	11
Figure 2. Producing reaction of poly(1-butene) [8].....	11
Figure 3. The chemical structure of the isotactic poly(1-butene) [12]	12
Figure 4. Definition of the dihedral angles in PB-1 [9].....	13
Figure 5. 3/1 helix packing in form I. Pair of isoclined helices:.....	15
Figure 6. Projection of the structure of PB-1 form II on the (001) plane [9]	16
Figure 7. Projection of the structure of PB-1 form III on the (001) plane as determined by X-ray diffraction. Only carbons are represented. Black and white marked carbons experience different local environments [9]	17
Figure 8. AFM height (a,c) and phase (b,d) images illustrates the two different kinds of PB-1 spherulites. The specimen was heat-treat at 160 °C for 5 min and then quenched to room temperature in air. [18]	19
Figure 9. Schematics showing routes for the formation and transformation of crystal modifications on crystallization and drawing of PB-1 [5].....	21
Figure 10. Transformation of crystalline form II → I of PB-1 produced by LyondellBasell [8].....	23
Figure 11. Dependence of transformation of form II → I of PB-1 on temperature and pressure [8]	23
Figure 12. Tensile behavior of PB-1 vs. other polyolefins [7]	26
Figure 13. Bragg's law [30].....	29
Figure 14. Generalized stress-strain curve that shows distinct yield [31].....	31
Figure 15. Single-screw plasticating extruder showing the four primary zones: hopper, solids feed, melting, and pumping [33]	32
Figure 16. Digital scale – KERN 770	38
Figure 17. Wide angle X-ray scattering patterns at different times [15]	39
Figure 18. PB 0300M – evolution of density in extrudates	42
Figure 19. DP 0401M – evolution of density in extrudates.....	43
Figure 20. PB 8640M – evolution of density in extrudates	43
Figure 21. Evolution of density in compression-molded specimens with thickness of 0.5 mm.....	44
Figure 22. Evolution of density in compression-molded specimens with thickness of 1 mm.....	45

Figure 23. Evolution of density in compression-molded specimens with thickness of 2 mm.....	45
Figure 24. PB 0300M – evolution of form I content	46
Figure 25. PB 0300M – evolution of tensile modulus in extrudates	48
Figure 26. DP 0401M – evolution of tensile modulus in extrudates	48
Figure 27. PB 8640M – evolution of tensile modulus in extrudates	49
Figure 28. Evolution of tensile modulus in injection-molded PB 0300M [43]	49
Figure 29. Evolution of tensile modulus in injection-molded DP 0401M [43].....	50
Figure 30. Evolution of tensile modulus in injection-molded PB 8640M [43]	50
Figure 31. PB 0300M – evolution of tensile yield strength in extrudates	52
Figure 32. DP 0401M – evolution of tensile yield strength in extrudates	53
Figure 33. PB 8640M – evolution of tensile yield strength in extrudates	53
Figure 34. Evolution of tensile strength at yield in injection-molded DP 0401M [43].....	54
Figure 35. PB 0300M evolution of tensile strength at break in extrudates	55
Figure 36. DP 0401M – evolution of tensile strength at break in extrudates	56
Figure 37. PB 8640M – evolution of tensile strength at break in extrudates	56
Figure 38. Evolution of tensile strength at break in injection-molded PB 0300M [43]	57
Figure 39. PB 0300M – evolution of tensile elongation at break in extrudates	58
Figure 40. DP 0401M – evolution of tensile elongation at break in extrudates	59
Figure 41. PB 8640M – evolution of tensile elongation at break in extrudates	59
Figure 42. Evolution of tensile elongation at break in injection-molded PB 0300M [43]	60

LIST OF TABLES

Table 1. Structural characteristics for the crystal modifications of PB-1 [5].....	14
Table 2. Density and melt temperature of PB-1	25
Table 3. Mechanical properties of PB-1 [7].....	26
Table 4. Basic properties of PB-1 grades [35]	35

LIST OF EQUATIONS

(1)	Bragg's law	29
(2)	Young's modulus	31